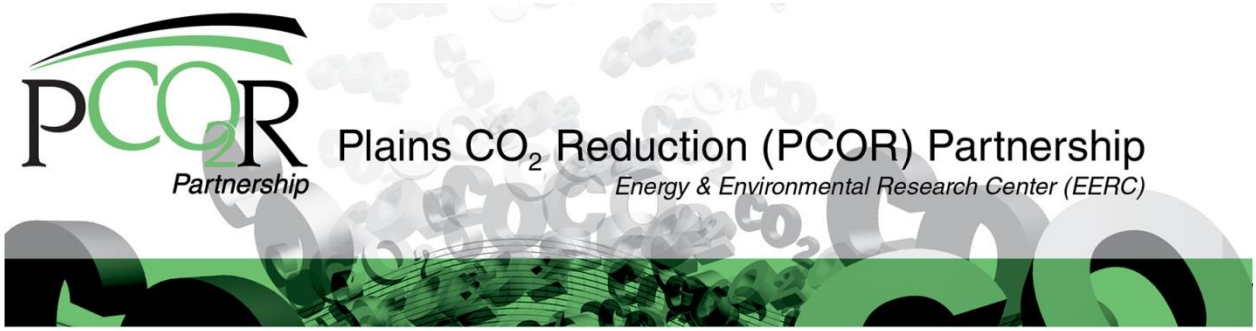

BELL CREEK FIELD TEST SITE – GEOMECHANICAL MODELING REPORT

Plains CO_2 Reduction (PCOR) Partnership Phase III
Task 9 – Deliverable D32

Prepared for:

Andrea T. McNemar

National Energy Technology Laboratory
U.S. Department of Energy
3610 Collins Ferry Road
PO Box 880
Morgantown, WV 26507-0880

DOE Cooperative Agreement No. DE-FC26-05NT42592

Prepared by:

Jun Ge
Robert C.L. Klenner
Guoxiang Liu
Jason R. Braunberger
Scott C. Ayash
Hui Pu
Panqing Gao
Terry P. Bailey
John A. Hamling
James A. Sorensen
Charles D. Gorecki
Edward N. Steadman
John A. Harju

Energy & Environmental Research Center
University of North Dakota
15 North 23rd Street, Stop 9018
Grand Forks, ND 58202-9018

January 2013
Approved

2016-EERC-02-18

EERC DISCLAIMER

LEGAL NOTICE This research report was prepared by the Energy & Environmental Research Center (EERC), an agency of the University of North Dakota, as an account of work sponsored by the U.S. Department of Energy (DOE) National Energy Technology Laboratory (NETL). Because of the research nature of the work performed, neither the EERC nor any of its employees makes any warranty, express or implied, or assumes any legal liability or responsibility for the accuracy, completeness, or usefulness of any information, apparatus, product, or process disclosed or represents that its use would not infringe privately owned rights. Reference herein to any specific commercial product, process, or service by trade name, trademark, manufacturer, or otherwise does not necessarily constitute or imply its endorsement or recommendation by the EERC.

ACKNOWLEDGMENT

This material is based upon work supported by the DOE NETL under Award Number DE-FC26-05NT42592.

DOE DISCLAIMER

This report was prepared as an account of work sponsored by an agency of the United States Government. Neither the United States Government, nor any agency thereof, nor any of their employees, makes any warranty, express or implied, or assumes any legal liability or responsibility for the accuracy, completeness, or usefulness of any information, apparatus, product, or process disclosed, or represents that its use would not infringe privately owned rights. Reference herein to any specific commercial product, process, or service by trade name, trademark, manufacturer, or otherwise does not necessarily constitute or imply its endorsement, recommendation, or favoring by the United States Government or any agency thereof. The views and opinions of authors expressed herein do not necessarily state or reflect those of the United States Government or any agency thereof.

NDIC DISCLAIMER

This report was prepared by the EERC pursuant to an agreement partially funded by the Industrial Commission of North Dakota, and neither the EERC nor any of its subcontractors nor the North Dakota Industrial Commission (NDIC) nor any person acting on behalf of either:

(A) Makes any warranty or representation, express or implied, with respect to the accuracy, completeness, or usefulness of the information contained in this report or that the use of any information, apparatus, method, or process disclosed in this report may not infringe privately owned rights; or

(B) Assumes any liabilities with respect to the use of, or for damages resulting from the use of, any information, apparatus, method, or process disclosed in this report.

Reference herein to any specific commercial product, process, or service by trade name, trademark, manufacturer, or otherwise does not necessarily constitute or imply its endorsement, recommendation, or favoring by the North Dakota Industrial Commission. The views and opinions of authors expressed herein do not necessarily state or reflect those of the North Dakota Industrial Commission.

ACKNOWLEDGMENT

The Plains CO_2 Reduction Partnership team would like to acknowledge Mehdi Ostadhassan for his efforts on behalf of this report. Mr. Ostadhassan is currently a graduate student at the University of North Dakota. We would also like to thank Dr. Dayanand Saini, who is no longer employed at the EERC, for his efforts contributing to this report.

TABLE OF CONTENTS

LIST OF FIGURES

Continued…

LIST OF FIGURES (continued)

LIST OF TABLES

BELL CREEK FIELD TEST SITE – GEOMECHANICAL MODELING REPORT

EXECUTIVE SUMMARY

The Plains CO_2 Reduction Partnership, led by the Energy & Environmental Research Center, is working with Denbury Resources Inc. to evaluate the effectiveness of large-scale injection of carbon dioxide (CO_2) into the Bell Creek oil field for simultaneous CO_2 enhanced oil recovery and long-term CO_2 storage. Site characterization activities for the Bell Creek Field are currently under way, including one-dimensional (1-D) and three-dimensional (3-D) geomechanical modeling. The comprehensive scope of this work includes building multidimensional, static geomechanical models as well as performing dynamic simulations using site-specific data. Information gained from this work can be used to assess various potential injection schemes; guide strategies for the monitoring, verification, and accounting (MVA) of the injected CO_2; predict geomechanical changes to the reservoir as a result of injection activities; better understand performance of the reservoir for both production and storage; predict potential risk scenarios; and provide insight into the ultimate fate of injected CO_2.

A 1-D mechanical earth model (MEM) was constructed based on existing data as well as field and laboratory data from a monitoring well (05-06 OW) drilled in December 2011. Preliminary analyses using the 1-D MEM include estimation of predrilling wellbore stability and stress polygons for determining the faulting regimes within the reservoir.

Key results of this work include the following.

Horizontal Stresses – Caliper logs helped to determine the orientations of horizontal stresses in the region immediately surrounding the monitoring well. The orientations of the maximum and minimum horizontal stresses are north–northeast–south–southwest and northwest–north–southeast–south, respectively. It should be noted that the magnitudes of these stresses in the region surrounding the well are nearly equal. This is further supported by only slight wellbore deformations that were observed (the greater the difference in magnitude between these stresses, the higher the probability for large wellbore deformation and breakouts). The acquisition of additional data and construction of the 3-D MEM will help approximate these stresses throughout the rest of the field.

Wellbore Stability Analysis – Based on the current 1-D MEM, created based on data collected from the monitoring well drilled in December 2011, the safe and stable mud weight windows were determined. The estimated maximum mud weight is 11.0567 pounds per gallon. No wellbore breakout will happen within the stable mud window, and this is corroborated by the fact that no breakouts have been found in the reservoir to date.

Induced Faulting – Preliminary stress polygon computations indicate that potential breakout through the reservoir as a result of drilling is extremely low.

A 3-D MEM, which incorporates the entire Bell Creek Field, is currently being constructed and will be completed when additional well logs and seismic data become available. Following the completion of the 3-D MEM, a comprehensive geomechanical analysis will be performed to identify, anticipate, and evaluate predrilling wellbore stability, cap rock integrity, the potential for induced fracturing or faulting, and the potential risk for out-of-zone fluid migration. It will also be used to match, monitor, and predict the geomechanical response from the reservoir and overlying formations and at the surface. Additionally, predictive geomechanical simulations will be designed and performed that will help guide and update the MVA plan, evaluate potential risk scenarios, and ensure injected CO_2 remains stored within the reservoir.

BELL CREEK FIELD TEST SITE – GEOMECHANICAL MODELING REPORT

INTRODUCTION

The Plains CO_2 Reduction (PCOR) Partnership, led by the Energy & Environmental Research Center (EERC), is working with Denbury Resources Inc. (Denbury) to determine the effect of large-scale injection of carbon dioxide (CO_2) into a deep clastic reservoir for the purpose of simultaneous CO_2 enhanced oil recovery (EOR) and CO_2 storage at the Bell Creek oil field, which is owned and operated by Denbury.

A technical team that includes Denbury, the EERC, and others is conducting a variety of activities to determine baseline reservoir characteristics. Among these activities, geomechanical modeling is being performed to 1) determine the geomechanical properties of the target injection formation and key sealing formations in the vicinity of the injection site and 2) simulate the effects that large-scale injection of CO_2 may have on geomechanical properties during injection and thereafter. This information can be used to assess various potential injection schemes, guide monitoring strategies, better understand performance of the reservoir, predict potential risk scenarios, and provide insight into the ultimate fate of injected CO_2.

This report summarizes the current work that has been done with respect to the geomechanical modeling for the Bell Creek project, including preliminary results, and outlines ongoing and future work.

BELL CREEK COMBINED EOR AND CO_2 STORAGE PROJECT OVERVIEW

The Bell Creek oil field in southeastern Montana is a significant hydrocarbon accumulation that lies near the northeastern corner of the Powder River Basin (Figure 1). Exploration and production activities for mineral and energy resources in the area over the last 55 years have yielded a significant amount of information about the geology of southeastern Montana and the northern portion of the Powder River Basin. Decades of oil and gas production through primary and secondary recovery (waterflood and polymer flood pilot tests) have resulted in approximately 38% recovery of the original oil in place (OOIP) and have left behind millions of barrels of oil, which is the target of a CO_2 injection-based tertiary oil recovery project. Fifty million cubic feet per day (ft^3/day) of CO_2 will be delivered to the site via pipeline from the ConocoPhillips Lost Cabin Gas Plant (Figure 1).

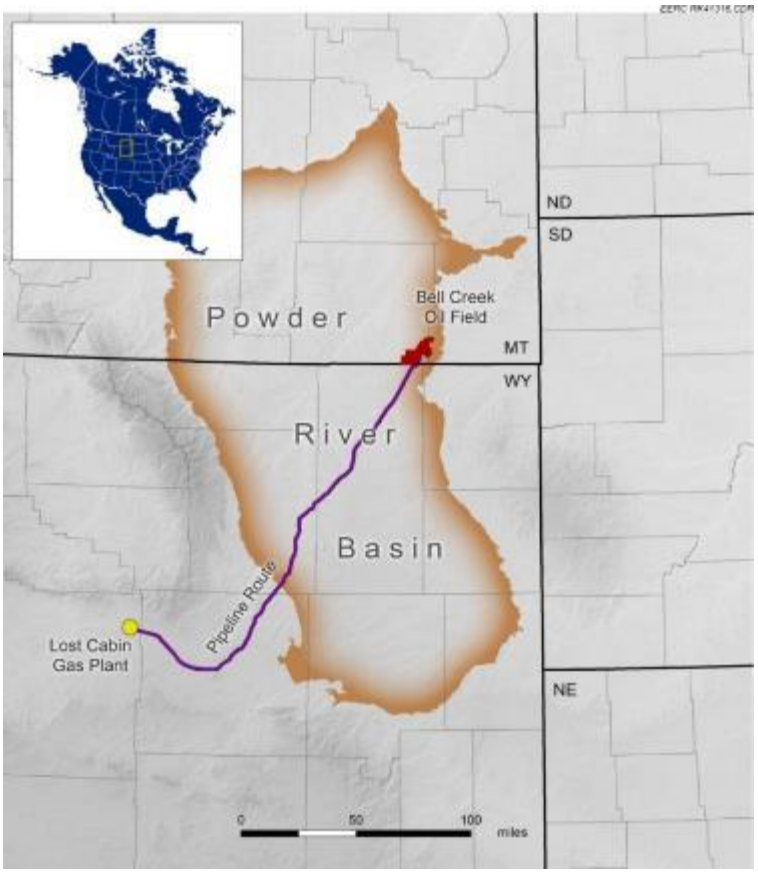

Figure 1. Map depicting the location of the Bell Creek oil field in relation to the Powder River Basin and the pipeline route from the Lost Cabin Gas Plant to the site.

CO_2 will be injected into the oil-bearing sandstone reservoir in the Lower Cretaceous Muddy Formation at a depth of approximately 4500 feet (Figure 2). CO_2 injection will occur in a staged approach (nine planned CO_2 development phases) across the field (Figure 3). It is expected that a miscible flood will be implemented at the Bell Creek Field, with at least 30 million barrels of incremental oil recovery. The activities at the Bell Creek oil field will inject an estimated 1.1 million tons of CO_2 annually, much of which will be permanently stored at the end of the EOR project.

Denbury will carry out the injection and production operations, while the EERC will provide support for site characterization, modeling and simulation work, and integrated risk assessment and aid in the development of the monitoring, verification, and accounting (MVA) plan to address key technical subsurface risks. The Bell Creek project will be a significant opportunity to develop a set of cost-effective MVA protocols for large-scale (>1 million tons a year) CO_2 storage associated with an EOR operation. The effectiveness of the MVA activities will be at least partially dependent on developing a thorough understanding of the geomechanical properties of the site. As a result, geomechanical characterization efforts will be designed to confirm the mechanical integrity of the system and are considered to be critical elements of the MVA program.

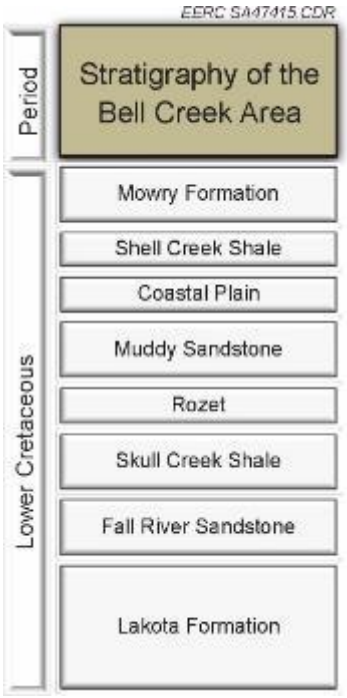

Figure 2. Stratigraphic column of the Lower Cretaceous period. The Bell Creek area column contains the nomenclature used in this report.

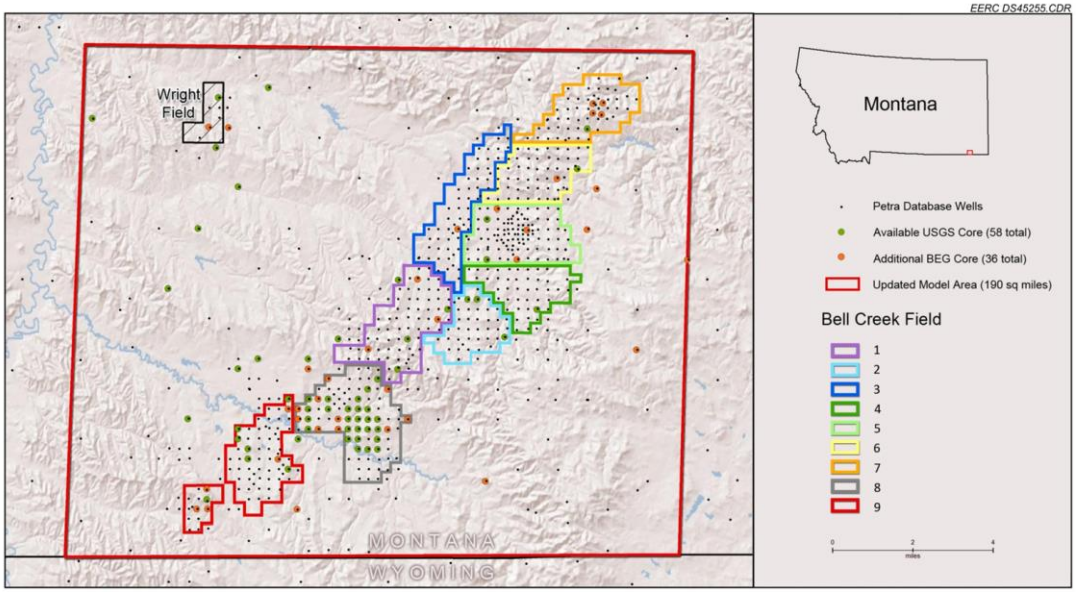

Figure 3. Bell Creek project development Phases 1–9 (USGS stands for U.S. Geological Survey. BEG stands for Bureau of Economic Geology at the University of Texas at Austin).

GEOLOGY OF THE BELL CREEK AREA

The regional stratigraphy consists of, in descending order, the Fort Union Formation, Hell Creek Formation, Fox Hills Formation, Pierre Formation, Shannon Formation, Niobrara Formation, Mowry Formation, Muddy Formation, Skull Creek Formation, and Lakota Formation (Figure 4). There are several other formations below the Lakota Formation, but those are not of primary interest and are not discussed in this report. Hydrocarbon accumulations are found in the oil-bearing sandstone reservoir in the Lower Cretaceous Muddy (Newcastle) Formation at a depth of approximately 4500 feet.

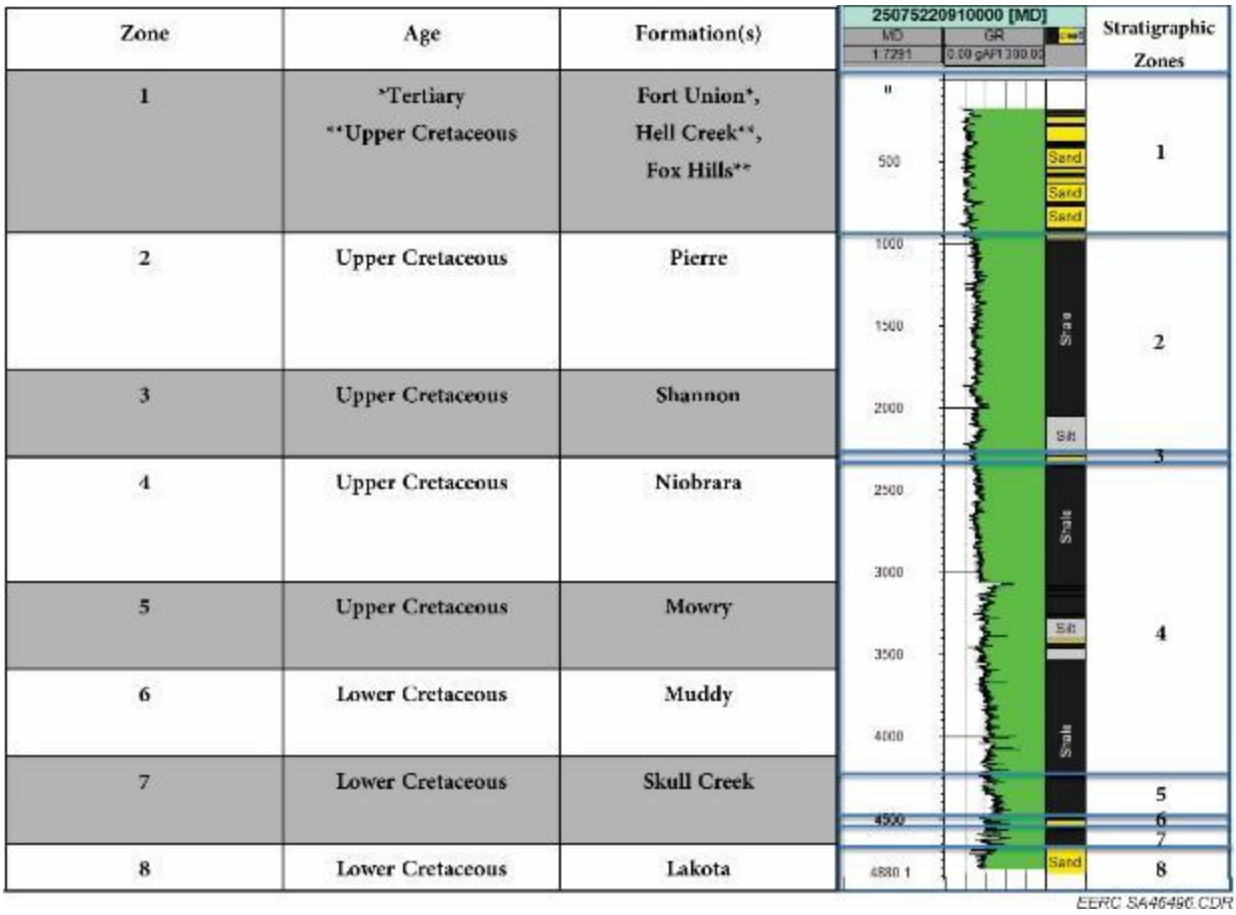

Figure 4. Gamma ray log from Well 25075220910000 in the Phase 1 area. Eight stratigraphic zones are denoted in descending order.

Within the Bell Creek oil field, the Muddy Formation ranges between 0 and 65 feet thick and comprises overlapping barrier bar sandstones deposited in a nearshore marine environment. The prominent, clean sandstones have favorable reservoir properties, with an average porosity of 24% and average permeability of 900 millidarcies (mD) (Table 1). The oil field is located structurally on a shallow monocline with a 1°–2° dip to the northwest. The barrier bar sand bodies of the Muddy Formation strike southwest to northeast for a distance of approximately 20 miles

and are partially dissected and somewhat compartmentalized by intersecting shale-filled incisive erosional channels.

Stratigraphically, the Muddy Formation in the Bell Creek oil field features an updip facies change from nearshore marine sandstone to offshore marine shale that serves as a trap for hydrocarbon accumulation and provides an effective seal for CO_2 injection. The overlying Upper Cretaceous Mowry Formation will provide the primary seal, preventing fluid migration to overlying aquifers and to the surface. Above the Mowry Formation is several thousand feet of low-permeability shale formations with a few thin layers of siltstone and sandstone (Figure 4) that will provide redundant layers of protection from upward migration of fluids. The Skull Creek Formation below the Muddy is also a low-permeability shale formation that will act as a seal. Thus, with the presence of both upper and lower seals, the injected CO_2 is expected to remain contained within the Muddy Formation.

GEOMECHANICAL MODELING

Objectives

Successful development for CO_2 storage and EOR operations requires a comprehensive understanding of the geomechanical responses of rock strength, pore pressure, in situ stress, and elastic properties caused by the injection and production of the reservoir. Drilling through the formation will cause stress alteration around the borehole and radially into the formation. The underground geomechanical processes associated with CO_2 injection are complex, and any changes in reservoir pressure and temperature can induce stress and strain changes in the reservoir formations around the injection zone. These changes may result in noticeable changes in permeability and injectivity and could, in extreme cases, lead to detectable seismic activity. If reservoir pressure becomes sufficiently high, more substantial, irreversible processes can occur, e.g., creation of new fractures, deformation of the well assembly, or reactivation of larger faults within the reservoir in the cap rock or overburden (Figure 5, modified from Rutqvist, 2008). The geomechanical modeling activities for the Bell Creek project have been designed to anticipate these changes within the reservoir in order to guide an injection strategy that will mitigate potential issues. A good estimation of formation elastic properties through geomechanical modeling will lead to an accurate stress analysis that can guide and inform the MVA plan as well as assist in assessing risk associated with CO_2 injection. For such reasons, geomechanical modeling is a crucial step for a better understanding of the reservoir system in conjunction with CO_2 storage and EOR.

Table 1. Key Characteristics of the Target Injection Formation

Formation	Depth, ft	Thickness, ft	Permeability, mD	Porosity, %
Muddy	4300–4600	0–65*	425–1175	25–35

* Although there are areas within the Bell Creek Field where the Muddy Formation pinches out to near-zero thickness, this does not negatively affect its suitability as a target for CO_2 EOR or storage operations.

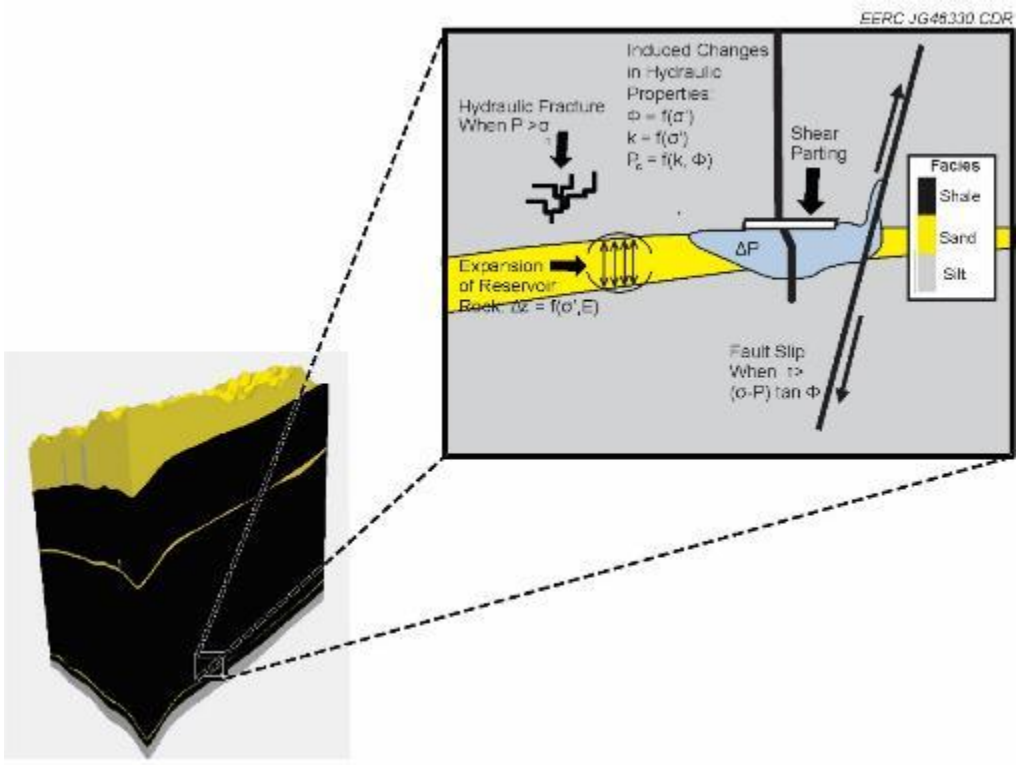

Figure 5. Geomechanical processes in CO_2 storage (modified from Rutqvist, 2008).

The objectives of the geomechanical modeling work for the Bell Creek combined CO_2 EOR and storage project include:

- Conducting a series of tests and analyses to determine the stress regime and rock mechanical properties for the reservoir formations and cap rock, including all of the overbearing formations to the surface.

- Performing an in-depth review of the structural features in the reservoir area to identify any existing faults or fractures.

- Predicting the stress variations during and after injection activities in order to verify the integrity of the cap rock and prevent existing fault reactivation with the desired injectivity.

- Simulating the deformation of the formation rocks to provide more accurate estimation of reservoir property variations due to geomechanical effects.

- Providing insight and direction for the MVA plan.

- Assisting with future interpretations of monitoring data.

Methods

In order to accomplish the objectives of the Bell Creek project geomechanical modeling, the work was divided into three main steps (Figure 6 shows steps in workflow format):

1. *Data Collection:* This step involves acquiring data from existing well logs, seismic data, and core analysis data.

2. *Mechanical Earth Model (MEM) Construction*: A static geomechanical model (the MEM) is constructed based on the available data. The creation of the MEM involved a staged approach, beginning with a one-dimensional (1-D) model and eventually progressing to a three-dimensional (3-D) model, with the acquisition of site characterization data. Figure 7 shows a flowchart outlining the stages of MEM development.

3. *Dynamic Simulation*: Coupled simulation using reservoir and geomechanical simulators is performed to achieve a comprehensive analysis of the reservoir system.

The completion of the 3-D MEM and the third step of performing dynamic geomechanical simulations constitute the future work outlined later in this report.

Completed Work

Because of the history of oil production in the Bell Creek Field, existing geologic data were readily available. Data were collected from existing well logs, 2-D seismic data, and laboratory core testing. In December 2011, a monitoring well (05-06 OW) was drilled in the Bell Creek Field. This well will be used for the purpose of monitoring the CO_2 flood of the Muddy Formation as part of the overall MVA program for the Bell Creek project. A permanent downhole-monitoring system was installed in the monitoring well to provide real-time pressure and temperature data. These pressure and temperature data were used to correlate log data. The drilling of the monitoring well allowed for the collection of additional data, both laboratory- and field-based. Laboratory-based activities included subjecting core plug samples to compression tests to determine rock strength, static and dynamic elastic properties, compressibility, and stress-dependent permeability. Field-based activities for the monitoring well included log-based analysis of in situ stress orientation and magnitude as well as rock mechanical properties. The results generated by the laboratory and field investigations provided the basis for the geomechanical modeling, specifically the basis for the 1-D and 3-D MEMs. In 2012, a 3-D seismic survey was conducted over an area of 41 square miles (mi^2) of the Bell Creek Field, and the processed data will be available in the near future for incorporation into the 3-D MEM (see Future Work for a discussion of the 3-D MEM).

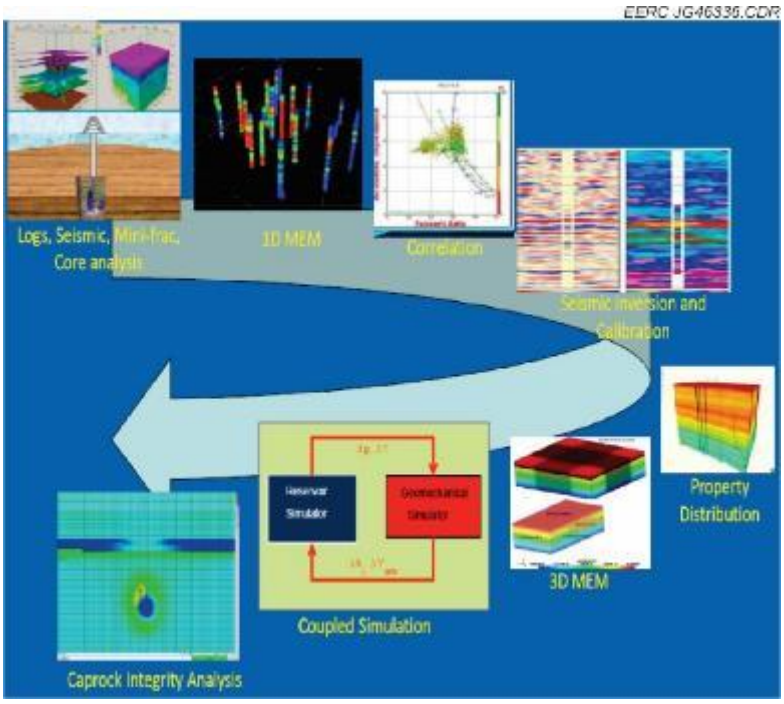

Figure 6. General geomechanical modeling workflow (Khan and others, 2010).

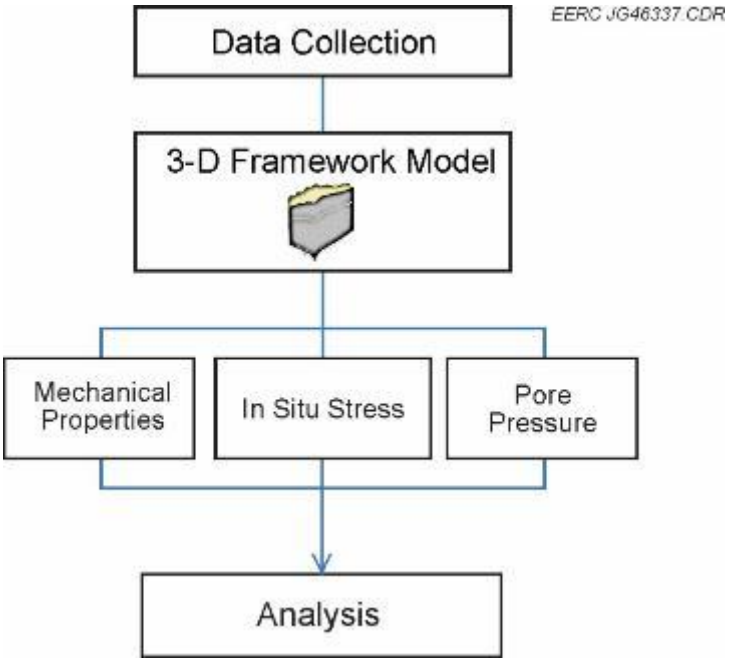

Figure 7. Flowchart for building a MEM.

The following activities based on the geomechanical modeling workflow have been completed:

- Sets of 1-inch-diameter core samples representing the cap rock and reservoir of the Bell Creek site were tested for bulk density, acoustic velocity, uniaxial strength, and triaxial strength. Elastic properties that were measured included confining stress at failure, peak strength, Young's modulus, Poisson's ratio, bulk modulus, and shear modulus.

- Logs from the monitoring well were collected and processed for mechanical properties, and the data have been incorporated into the geomechanical model.

- Log data were quality-checked and used to build the 1-D MEM along the monitoring well.

- The monitoring well log data, along with available log data from other wells in the field, were correlated to provide more information for the future fieldwide 3-D MEM geomechanical model.

Mechancial Earth Model

The MEM is a numerical representation of the state of stress and rock mechanical properties for a specific stratigraphic section in a field (Plumb and others, 2000). The basic form of the MEM consists of depth profiles of elastic parameters, rock strength, and stresses. The model can be linked to a geologic structure through the local stratigraphy and a 3-D seismic cube (Plumb and others, 2000). The MEM can be built in one, two, or three dimensions, which is limited only by the available data. The 1-D MEM is built along wells in a field that have sufficient data to derive the rock mechanical properties and stress state.

Earth stresses vary with pore pressure changes during CO_2 injection activities and thus cause deformation of the reservoir and surrounding formations. This deformation can lead to wellbore failure or the reactivation of natural fractures, both of which can be detrimental to drilling and injection operations. The creation of a 1-D MEM can aid in the understanding of reservoir response to various stress states which can, in turn, allow for prediction of formation deformations, permeability variations, and the maximum injection rate and pressure that can be utilized without damaging the integrity of the reservoir and confining units.

A 1-D MEM has been created for the Muddy Formation and upper confining units in the Bell Creek oil field to assess the state of stress and reservoir mechanical properties in the area surrounding the 05-06 OW monitoring well. This analysis will be the basis for future 3-D geomechanical models.

1-D MEM Development

The development of a 1-D MEM follows a detailed workflow, as shown in Figure 8 (modified from Nagy and others, 2011). First, all available data, including geology, well logs, seismic, and lab testing, are collected and checked for quality. This step is necessary since the absence of data can increase the uncertainty in the model. The second step is to determine the

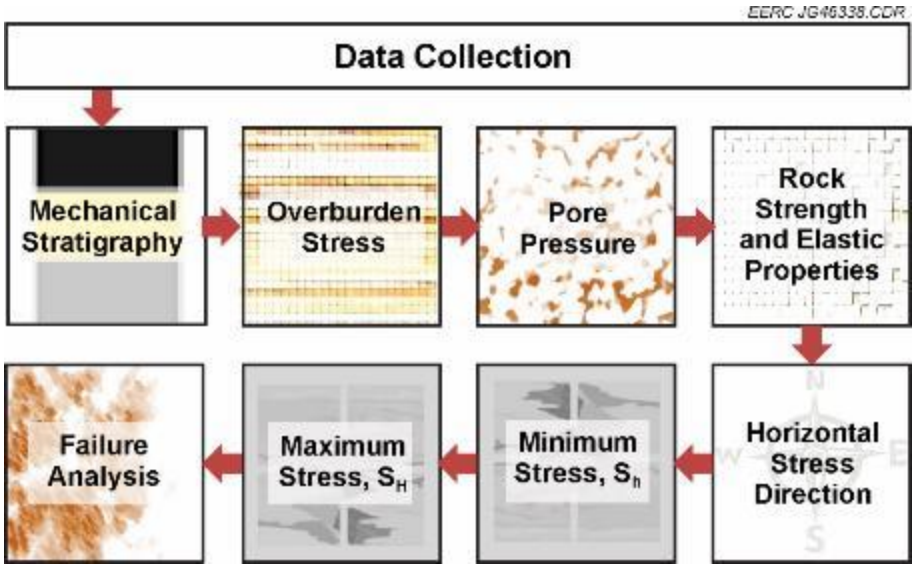

Figure 8. Detailed workflow for building the 1-D MEM (modified from Nagy and others, 2011).

mechanical stratigraphy for the model. The mechanical stratigraphy is the discrete zones and layers in the model, which provide information regarding facies and local deformation mechanisms. Once the mechanical stratigraphy is determined, the model can be populated with the mechanical properties and stress states of the system, which are derived from calculations and correlations of the available data. Finally, the 1-D MEM is used to perform a failure analysis for wellbore stability. This wellbore analysis can be used to instruct drilling operations and estimate the potential for leakage along the wellbore.

The 1-D MEM for the Bell Creek project was created from the 05-06 OW well logs (including both open and cased-hole logs), 2-D seismic data, and core rock mechanical properties obtained from laboratory testing. Logs that were incorporated into the 1-D MEM include GR (gamma ray), caliper, RHOB (bulk density), S_V (vertical stress), SH_{Max} and SH_{Min} (maximum and minimum horizontal stress), pore pressure, mud pressure, fracture initiation press, UCS (unconfined compressive strength), Poisson's ratio, Biot's coefficient, and Young's modulus. The log data were then analyzed in Schlumberger's Techlog and imported into Schlumberger's Petrel for the visualization of the 1-D MEM. Log data were correlated to laboratory and reservoir test results.

The log data were analyzed in Techlog for lithology analysis, pore pressure prediction, in situ stress analysis, and rock elastic properties. The lithology analysis was based on spectral GR logs, bulk density, neutron porosity, and sonic logs. The pore pressure prediction was done with an analysis of the sonic log and corrected using the pressure gauge data from the monitoring well. The in situ stresses and rock elastic properties were estimated from the sonic and bulk density logs as well as the empirical relationships between some of the properties. Appendix A contains a detailed description of the estimation of the rock elastic mechanical properties. The raw log curves from the monitoring well are displayed in Figure 9, which include GR, SP (spontaneous potential),

RHOB, DTC (compressive slowness), and DTS (shear slowness). These log curves were used to obtain the rock mechanical properties and stress states along the well.

Table 2 shows examples of the data that were derived from some of the available processed logs for the 05-06 OW well.

The goal for the Bell Creek geomechanical modeling efforts was to build a model from the Lakota Formation (Figure 4) through the Muddy Formation (target injection formation) to the surface. However the majority of available logs lack data for the depth range of 0 to 1254 ft because of surface casing interference. As a result, the 1-D MEM was built using the available data and ranges from depths of 1254 to 4732 ft, i.e., from the Pierre Formation to the Lakota Formation. In order to determine the vertical stress for the system, it was necessary to integrate bulk density from the surface to the depth of interest. The lack of data from 0 to 1254 ft required the extrapolation of the bulk density log over this range. This was done using an empirical equation (Equation 1, Sayers and others, 2009). The determined density trend from the monitoring is shown in Figure 10.

$$\rho(z) = \rho_0 + az^b \qquad \text{[Eq. 1]}$$

In conjunction with log data from the monitoring well, three core samples (47V, 50, and 49V) had triaxial compressive tests performed in April 2012. The results are shown in Tables 3 and 4. The stress–strain relations were analyzed for the three samples by Core Laboratories. Results appear in Figures 11–13.

Finally, in addition to log data and core testing, 2-D seismic data were available. These data were used to estimate the magnitude of the maximum horizontal stress and its correlation with the minimum horizontal stress in the reservoir (Appendix B). The generated P-wave velocity from the 2-D seismic was used to produce the S-wave velocity by Vp-Vs transform crossplots. The P and S waves were then modified with the velocity log data for the reservoir conditions, and the magnitude of the maximum horizontal stress was calculated by finding the three shear moduli with the P and S waves. The results of these calculations indicate that the magnitudes of the maximum and minimum horizontal stresses are approximately equal in the region around the monitoring well.

After data collection and verification, the 1-D MEM was constructed between the interval of 1254 to 4732 ft. The step depth was set to be 0.25 ft. However, because the step depth of the RHOB log was 0.5 ft, it was necessary to convert it to 0.25 ft in order for it to be used with the sonic data. This conversion process was done using Excel. The three samples from the core analysis triaxial test were used as a reference and for verification.

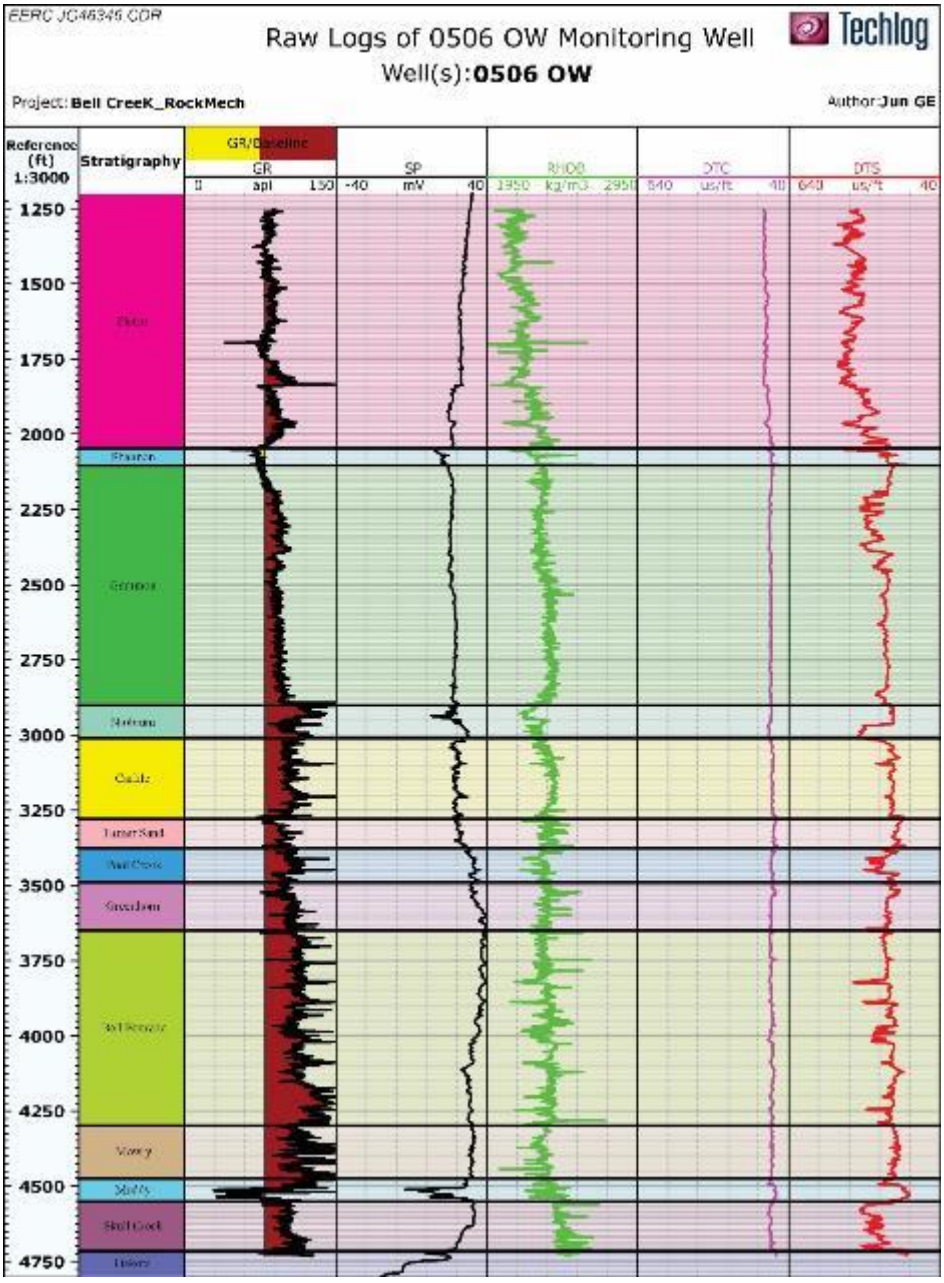

Figure 9. Raw log curves from the monitoring well.

Table 2. Assorted Logs and Their Corresponding Derived Data

Log	Data
Magnetic Resonance Image Log	Permeability, clay mineralogy, and porosity
Wave Sonic Travel Time	Elastic property stress calculations
X-Tended Range Micro Imager (XRMI™)	Wellbore deformation, breakouts, fractures, and stress determination

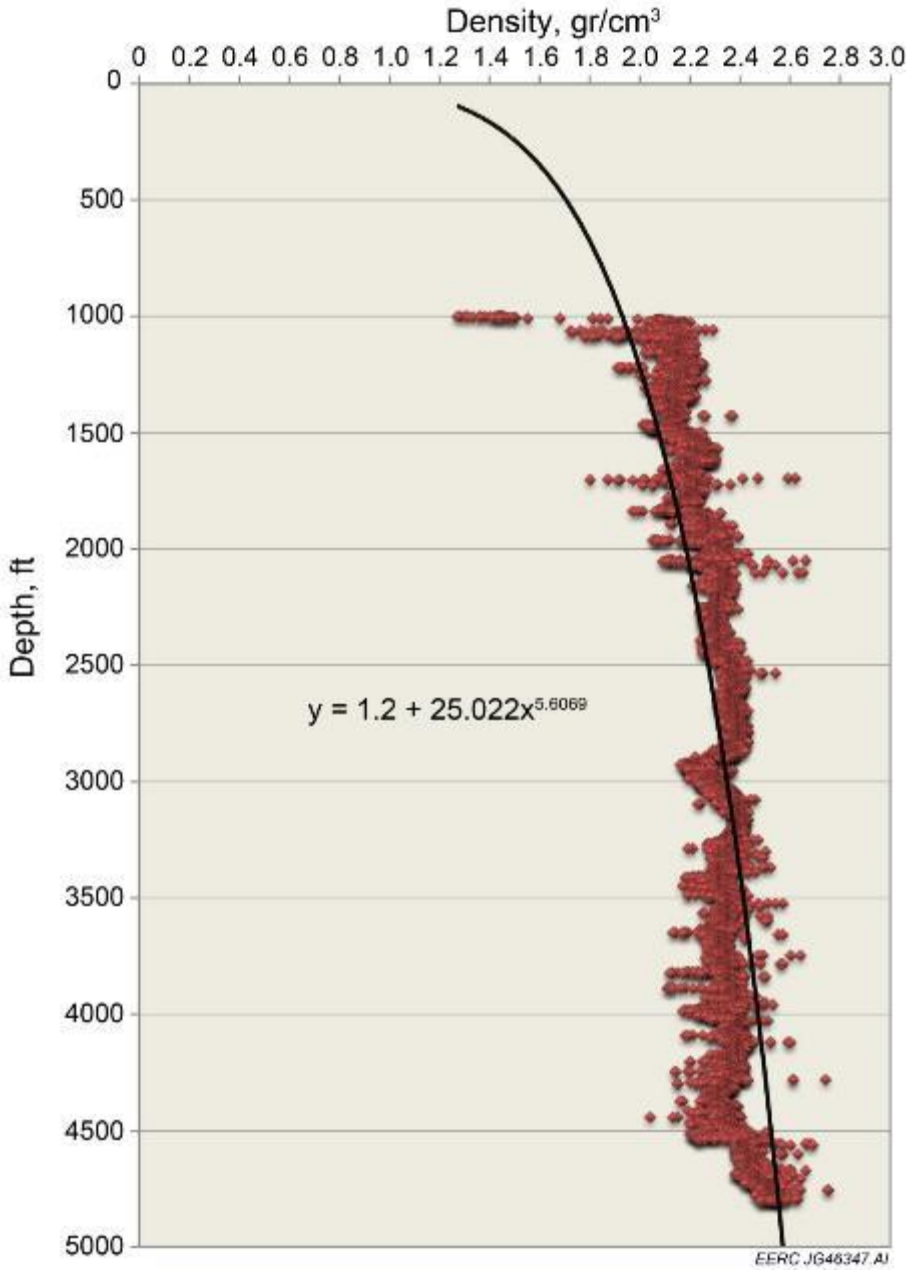

Figure 10. Density trend from the monitoring well.

Table 3. Triaxial Static Young's Modulus, Poisson's Ratio, and Compressive Strength

Sample No.	Depth, ft	Confining Pressure, psi	Bulk Density, gm/cm^3	Compressive Strength, psi	Young's Modulus, 10^6 psi	Poisson's Ratio
47V	4495.10	670	2.30	7625	1.10	0.20
50	4496.30	670	2.69	10,125	2.15	0.22
49V	4542.20	670	2.39	3853	0.28	0.20

Table 4. Acoustic Velocities and Dynamic Moduli at Triaxial Stress Conditions

Sample No.	Confining Pressure, psi	Axial Pressure, psi	Acoustic Velocity Compressional ft/sec	Compressional µs/ft	Shear ft/sec	Shear µs/ft	Young's Modulus, x10^6 psi	Shear Modulus, x10^6 psi	Poisson's Ratio
47V	670	670	8884	112.56	5326	187.77	2.15	0.88	0.22
	670	3670	9213	108.54	5457	183.25	2.27	0.92	0.23
50	670	670	14,238	70.24	8507	117.55	6.42	2.63	0.22
	670	5670	14,901	67.11	8650	115.60	6.77	2.72	0.25
49V	670	670	8994	111.18	5512	181.43	2.35	0.98	0.20
	670	1670	9433	106.02	5673	176.26	2.52	1.04	0.22

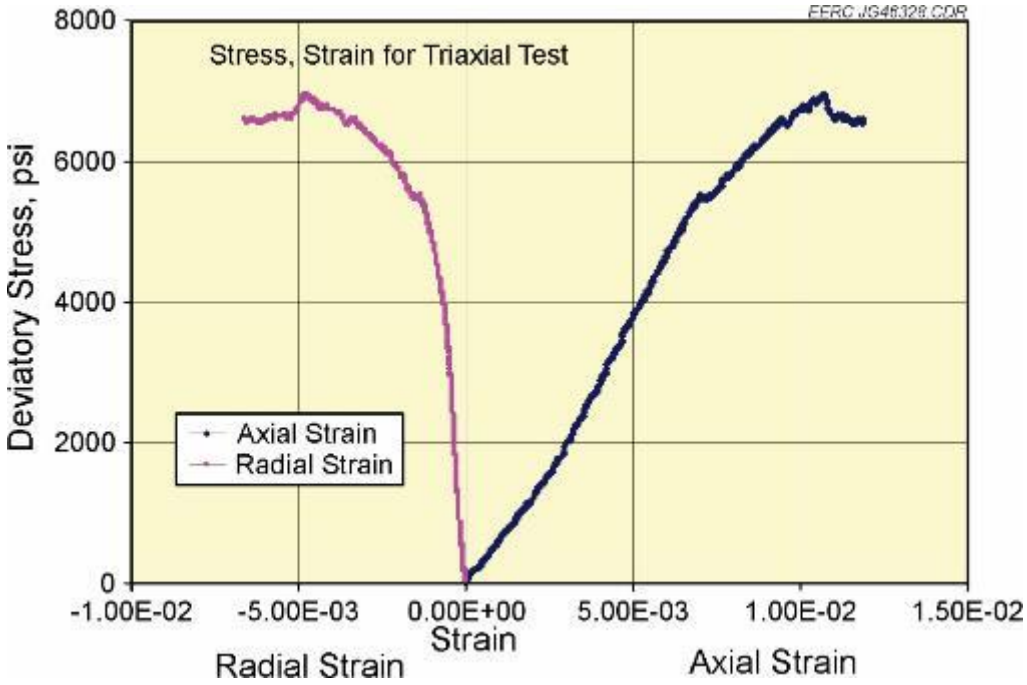

Figure 11. Stress–strain relationship for Sample 47V.

The first step for constructing the 1-D MEM was to estimate the in situ stress regime along the monitoring well. A detailed discussion of these estimations is contained in Appendix A. The vertical stress was calculated using the bulk density log. To calculate pore pressure along the monitoring well, the Eaton method (Eaton, 1969) was employed to estimate the pore pressure log. This pore pressure log was then compared with the pore pressure provided by the logging company that processed the log data and also adjusted using the pressure gauge data for the monitoring well. The magnitude of the minimum horizontal stress was determined by the elastic properties, v, E, and α (Biot's coefficient) by assuming zero strains. Biot's coefficient is provided by the processed logs. Normally, the XRMI image log can be used for the estimation of the magnitude of the maximum horizontal stress. However, no borehole breakouts or induced tensile fractures have been found in the XRMI image log. Because of the absence of borehole breakouts or induced

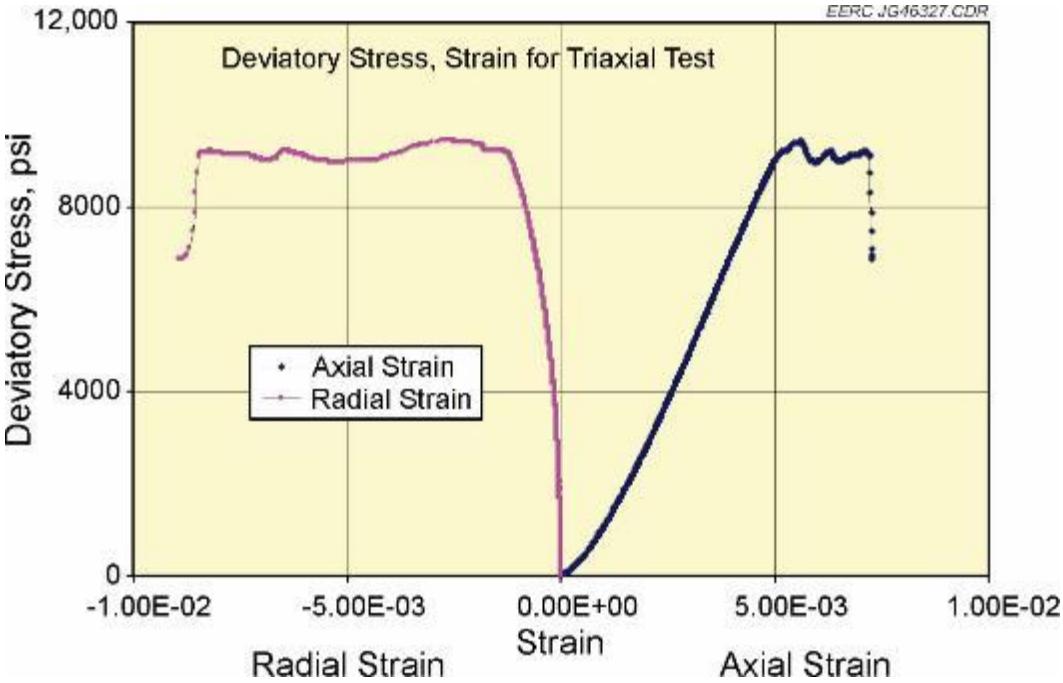

Figure 12. Stress–strain relationship for Sample 50.

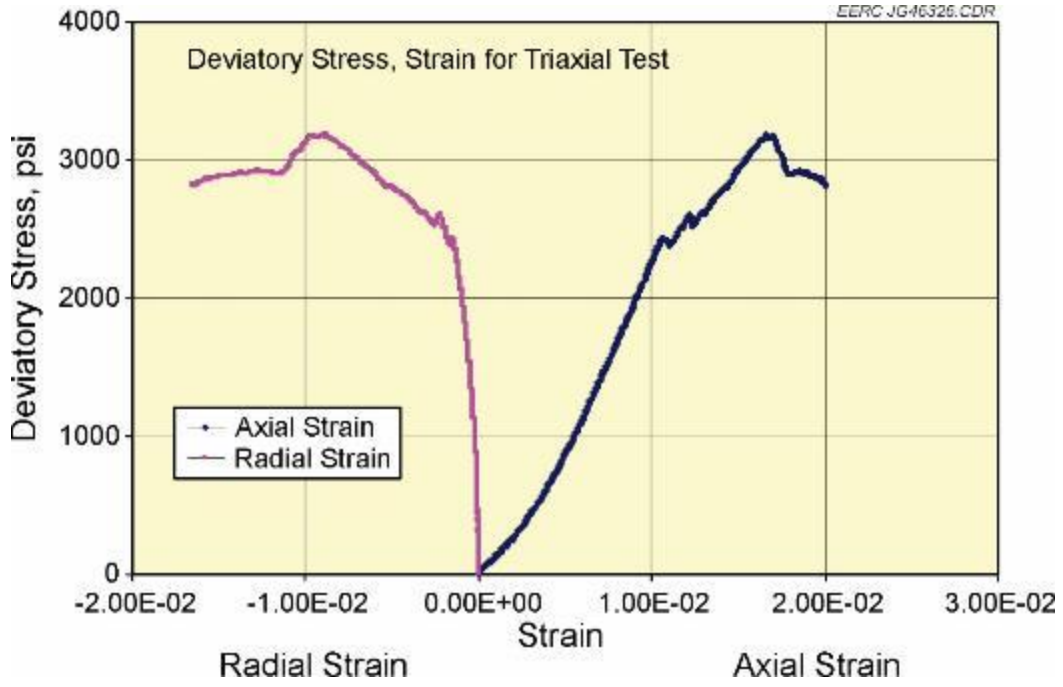

Figure 13. Stress–strain relationship for Sample 49V.

tensile factures, it was not possible to set up the constrain model for estimating the magnitude of the maximum horizontal stress. Based on the equations for the three shear moduli, the magnitude of the maximum horizontal stress in several reservoir layers was calculated (Appendix B, Table B-1). With these data, the tectonic stress was estimated for the Bell Creek Field, and the equation for hydraulic fracturing stress was used for the estimation of the magnitude of the maximum horizontal stress. The final rock properties and stress state for the 1-D MEM are shown in Figure 14.

The final step for the 1-D MEM was to determine the orientations for the horizontal stresses. Using caliper logs, it was possible to estimate the approximate directions of the horizontal stresses by observing slight deformations in the wellbore (Figure 15). Figure 16 shows the approximate orientation of the maximum and minimum horizontal stresses, i.e., north–northeast–south–southwest and northwest–north–southeast–south, respectively.

With the constructed properties logs, the 1-D MEM data were imported into Petrel within the framework of the Bell Creek geocellular model. An example can be seen in Figure 17, which shows the vertical principal stress along the monitoring well.

Results and Discussion

Table 5 shows the average values of the rock mechanical properties calculated from the sonic and bulk density logs acquired from the 05-06 OW monitoring well, as well as the depth based on mechanical stratigraphy, of each formation interval. The dynamic properties were calculated using the methods described in Appendix A, while the static Young's modulus and the UCS were derived using accepted correlations from the oil and gas industry. Although an estimate for Poisson's ratio was made, the correlation between static and dynamic Poisson's ratio is not straightforward.

Equation 2 shows a simplified correlation between the static and dynamic Poisson's ratio:

$$v_{sta} = C1 v_{dyn} + C2 \qquad \text{[Eq. 2]}$$

where C1 and C2 are constants that can be determined using triaxial test results with measured velocities. The static Poisson's ratio is very dependent on the values of these constants, particularly C1. Additionally, C1 and C2 can vary dramatically from test to test, even for the same type of rock. Typical industry models set C2 as 0, and C1 varies from 0.7 to 1.2.

For the 05-06 OW monitoring well, a value of 1.24 for C1 was assumed by the logging company. However, following discussion with the company, it was concluded that a C1 value of 1.24 may be too high, resulting in a poor estimate for the static Poisson's ratio of the first sealing formation—the Mowry Shale. Based on available literature (Crain 2013a,b; Gale and others 2007), the value of the static Poisson's ratio for shale is typically 0.1–0.45, with most U.S. shale formations between 0.2–0.4. For the 1-D MEM, the correlated constants from the triaxial test results of the Muddy Formation were used for C1 and C2 (0.714 for C1 and 0.044 for C2). These

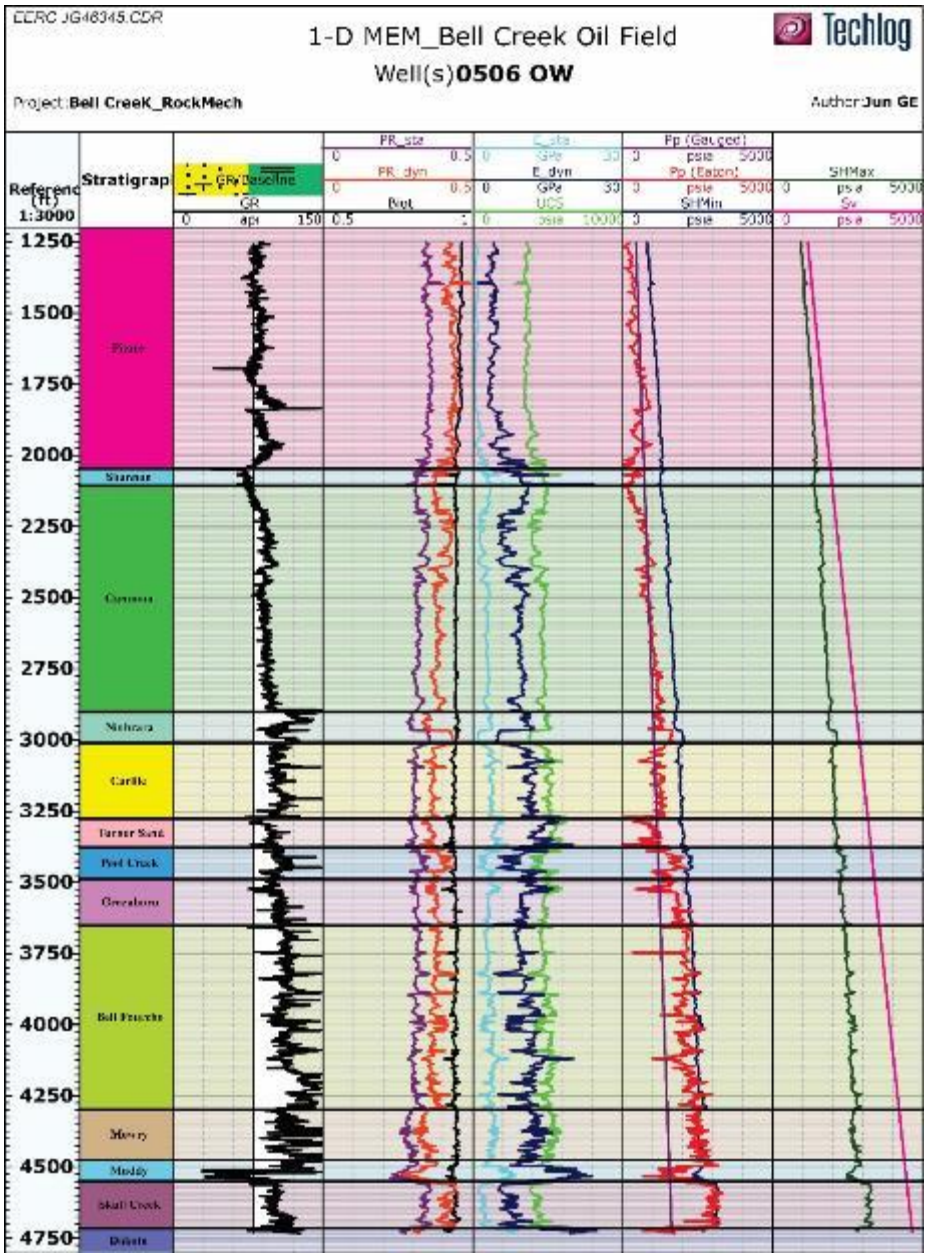

Figure 14. Properties of the 1-D MEM of the monitoring well.

values for C1 and C2 resulted in a range of 0.25 to 0.35 for the static Poisson's ratio (Table 5). The static Poisson's ratio calculated with C1 values of 1.0 and 1.24 (C2=0) are also shown in Table 5 for comparison.

It should be noted that values of C1 and C2 used for the 1-D MEM (i.e., 0.714 and 0.044 respectively) were derived from triaxial tests of the Springen Ranch and Rozet intervals of the Muddy Formation. The values for the static Poisson's ratio for the other formations shown in Table 5 are meant to be approximations only. The actual static Poisson's ratio for these formations should be substantiated by geomechanical tests on representative core samples.

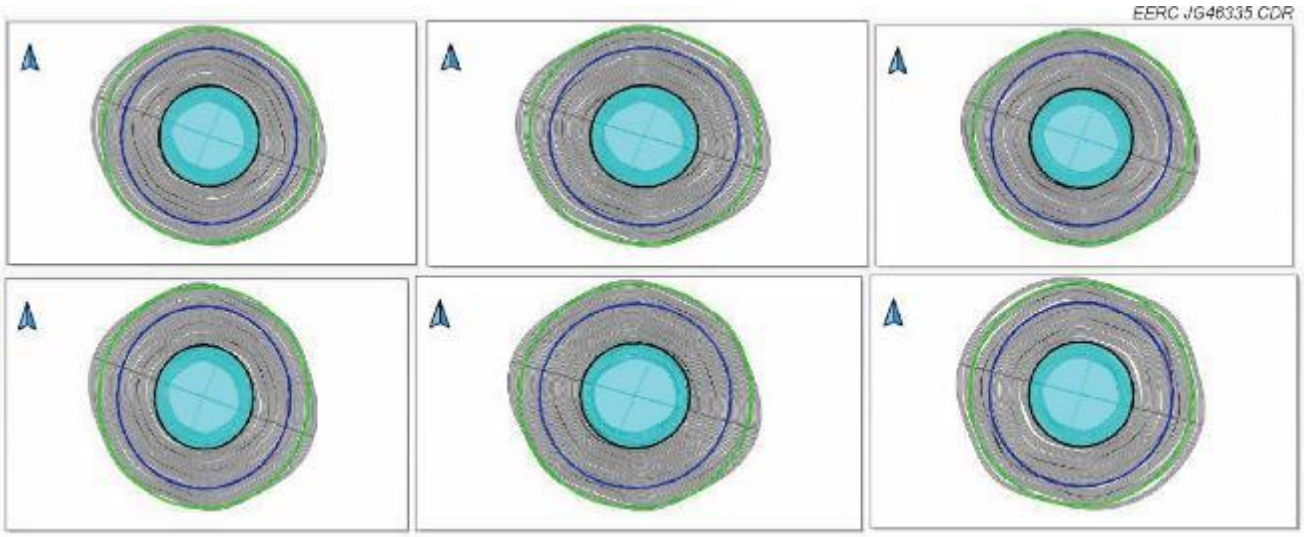

Figure 15. General wellbore deformation throughout the Muddy Formation.

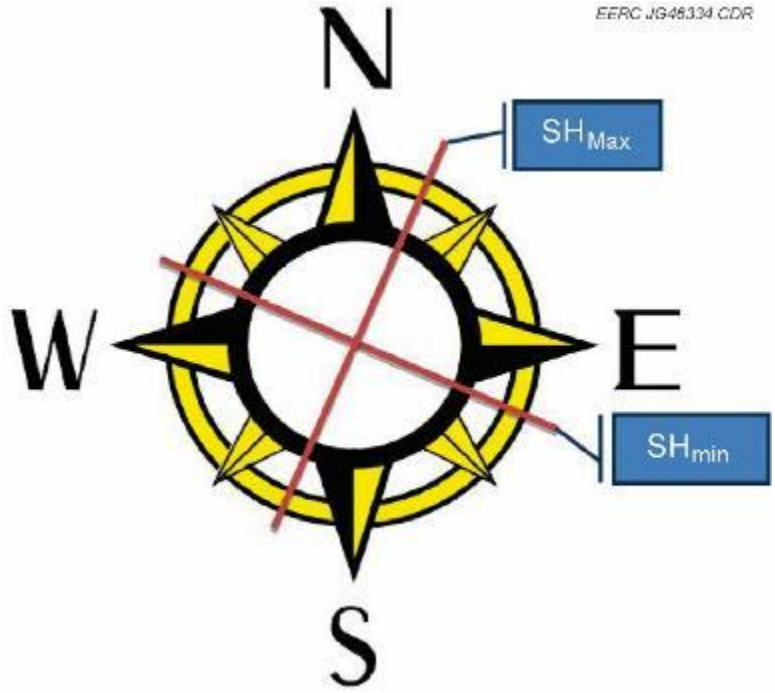

Figure 16. Estimation of the orientations of maximum (SH_{Max}) and minimum (SH_{Min}) horizontal stresses.

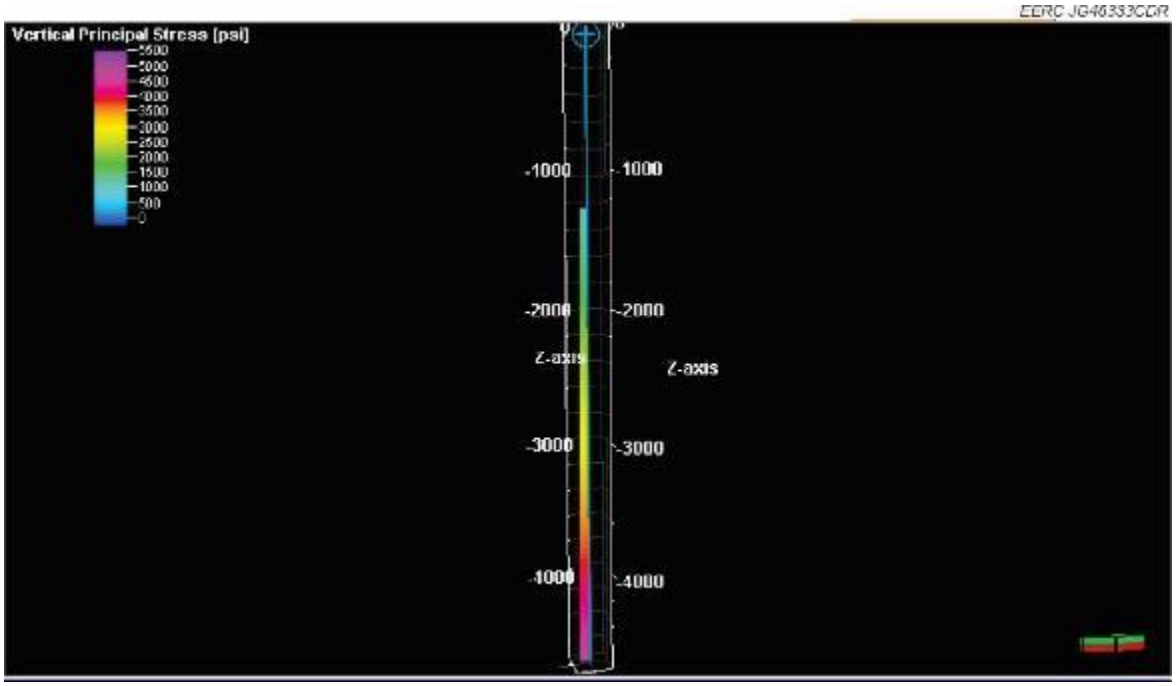

Figure 17. Vertical principal stress along the monitoring well (05-06 OW).

The constructed 1-D MEM was used to predict the wellbore stability in each formation along the wellbore. A safe and stable mud weight window, which is important for safe drilling, is located in the mud pressure range between the pore pressure and the minimum horizontal stress. If the mud pressure is less than the formation pore pressure, the drilling fluid will enter into the kick zone. If the mud pressure is greater than the minimum horizontal stress, the drilling activity will initiate induced fractures, causing mud loss in the well (Afasari and others, 2010). The mechanical stable mud window is located in the mud pressure range between minimum mud weight, i.e., shear failure or breakout mud weight, and maximum mud weight, i.e., tensile failure or breakdown mud weight. The equations for the lower and upper limits of mud weight are shown as follows (Afasari and others, 2010):

$$P_{mud} \geq 3\sigma_H - \sigma_h - P_p - UCS \quad \text{[Eq. 2]}$$

$$P_{mud} \leq 3\sigma_h - \sigma_H - P_p + T \quad \text{[Eq. 3]}$$

where P_{mud} is hydrostatic mud pressure, T is the tensile strength of the rocks, P_p is pore pressure, σ_H is maximum horizontal stress, σ_h is minimum horizontal stress, and UCS is unconfined compressive strength. For this analysis, tensile strength (T) was set to 0 psi to follow a "worst-case scenario" approach.

Table 5. Average Dynamic and Static Rock Mechanical Properties Derived for Each Formation

Formation	Depth, ft	Young's Modulus, GPa		Poisson's Ratio, ν			UCS, psia
		Dynamic	Static	Dynamic	Static*	Static**	
Pierre	1254.0–1849.5	3.91	0.56	0.43	0.35	0.50	3575
Eagle	1849.5–2048.0	5.79	1.34	0.42	0.35	0.50	3948
Shannon	2048.0–2105.0	9.55	2.90	0.38	0.32	0.48	4694
Gammon	2105.0–2901.0	8.77	2.58	0.39	0.32	0.48	4540
Niobrara	2901.0–3012.0	8.60	2.50	0.38	0.32	0.47	4505
Carlile	3012.0–3278.0	11.47	3.70	0.37	0.31	0.46	5075
Turner Sand	3278.0–3377.0	13.82	4.67	0.36	0.30	0.44	5541
Pool Creek	3377.0–3489.5	9.22	2.76	0.39	0.33	0.49	4629
Greenhorn	3489.5–3650.5	10.35	3.23	0.38	0.31	0.47	4853
Bell Fourche	3650.5–4297.5	10.47	3.28	0.38	0.31	0.47	4878
Mowry	4297.5–4475.5	12.43	4.09	0.34	0.29	0.42	5265
Shell Creek	4475.5–4490.0	10.42	3.26	0.37	0.31	0.45	4866
Springen Ranch	4490.0–4497.0	9.30	2.80	0.37	0.31	0.46	4645
CP	4497.0–4507.5	16.18	5.65	0.34	0.29	0.42	6009
BC Sand	4507.5–4538.0	19.72	7.12	0.30	0.26	0.37	6713
Rozet	4538.0–4550.5	14.90	5.12	0.35	0.29	0.43	5756
Skull Creek	4550.5–4716.0	7.83	2.19	0.41	0.34	0.51	4354

Notes:
Dynamic Poisson's ratio = static Poisson's ratio when C1=1 and C2=0
Static* = C1=0.714 and C2=0.044
Static** = C1=1.24 and C2=0

The 1-D MEM for the monitoring well was used to calculate the safe and stable mud weight window, which can be used as a guide for future drilling activities in the Bell Creek oil field. The gauge-modified pore pressure was used as the minimum safe mud weight, and the minimum horizontal stress was used as the maximum safe mud weight. For the breakout mud weight (Pmud_lower) pressure, the results from Equation 2 were always less than 0, indicating that no breakout will happen at any mud weight condition. The P_{mud} from Equation 3 was used as the maximum stable mud weight (Pmud_upper in Figure 18).

In order to avoid fracturing or formation breakdown, the maximum mud weight should be lower than the smaller value (either the maximum safe mud weight or the maximum stable mud weight). In the 1-D MEM, the maximum mud weight was estimated as less than the minimum horizontal stress or calculated from the following equation:

$$P_{mud\_max} = \frac{v}{1-v}\left(\sigma_v - \alpha P_p\right) + \alpha P_p \qquad \text{[Eq. 4]}$$

To estimate the maximum mud weight as a guide for future drilling activities, the pressure gradient, in situ stress gradients, average Poisson's ratio, and average Biot's coefficient were calculated from the 1-D MEM. The estimated maximum mud weight in pounds per gallon (ppg) is 11.0567 (Table 6). Two points should be noted: 1) there are no safety factors included in this value and 2) this value was estimated using average values based on limited data from only one

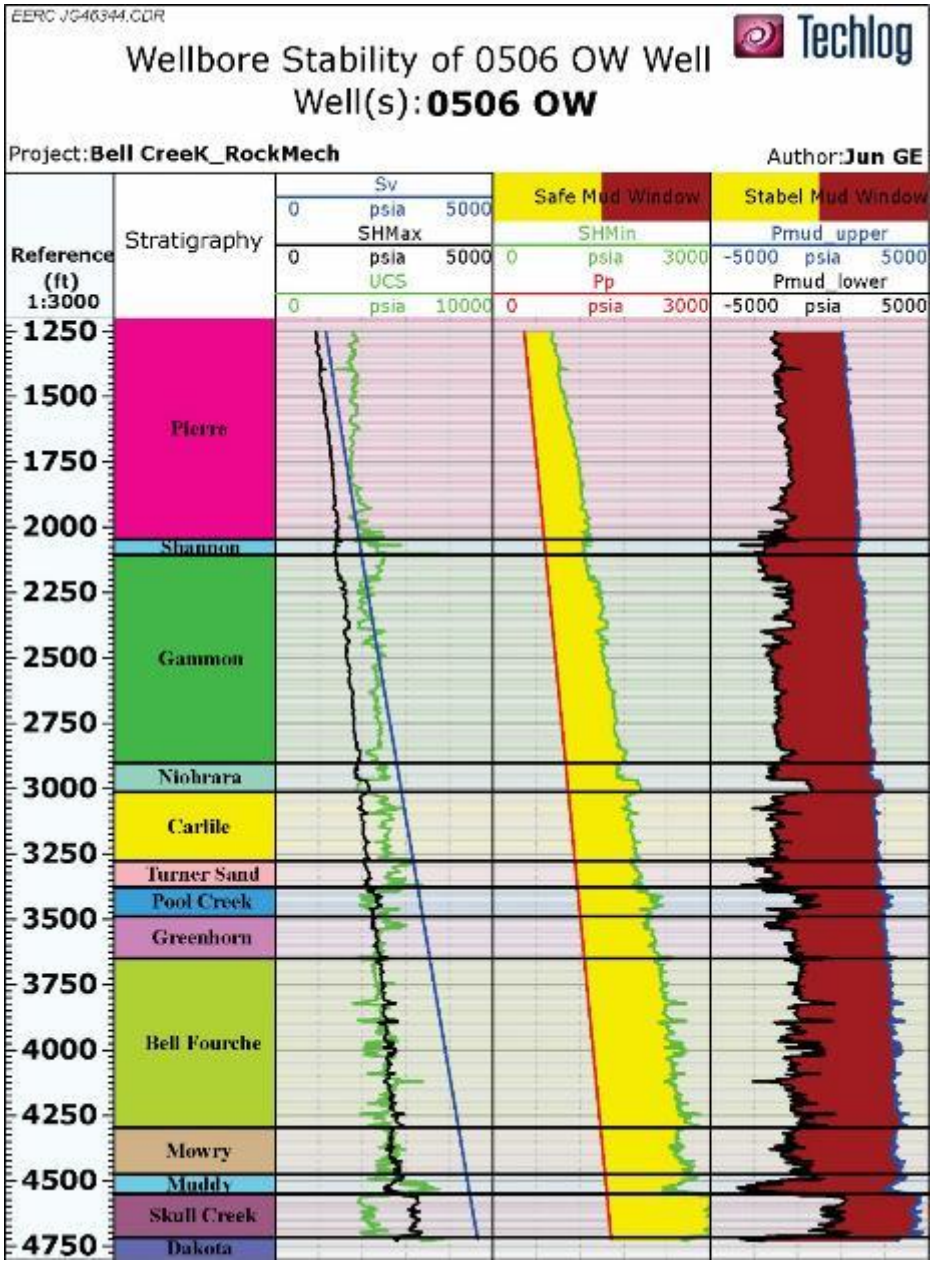

Figure 18. Wellbore stability analysis for the monitoring well based on the 1-D MEM.

Table 6. Pressure Gradient and Maximum Mud Weight

Pore Pressure Gradient, psi/ft	Vertical Stress Gradient, psi/ft	Average Poisson's Ratio	Average Biot's Coefficient	Maximum Mud Weight, ppg
0.345	1.010	0.267	0.944	11.0567*

* This value is based on a numerical analysis for one well. The actual mud weight for any new well drilled in the Bell Creek Field should be determined through drilling operations.

monitoring well. To provide more relevant fieldwide support for future drilling activities, additional data from leakoff tests, experimental data, and seismic data should be used to populate the fieldwide 3-D MEM.

In addition to the prediction for wellbore stability, the 1-D MEM was used to determine the faulting regime in the reservoir. The stress polygon at initial reservoir conditions and recent reservoir conditions was constructed to determine the faulting regime of natural fractures in the reservoir (Figures 19 and 20). At the initial reservoir stress conditions, stress polygon computation shows the potential for breakout through the reservoir section is extremely low (Figure 19). This is corroborated by the fact that no faulting has been identified in the reservoir to date.

While the results from the 1-D MEM analyses can provide some approximations to help guide future drilling, it is highly recommended that more data be collected and incorporated into the 3-D MEM in order to gain a more accurate understanding of the site-specific geomechanical factors that could affect drilling and well planning in the Bell Creek Field, e.g., changes in stress, strain, pressure, permeability, and porosity resulting from the injection of CO_2.

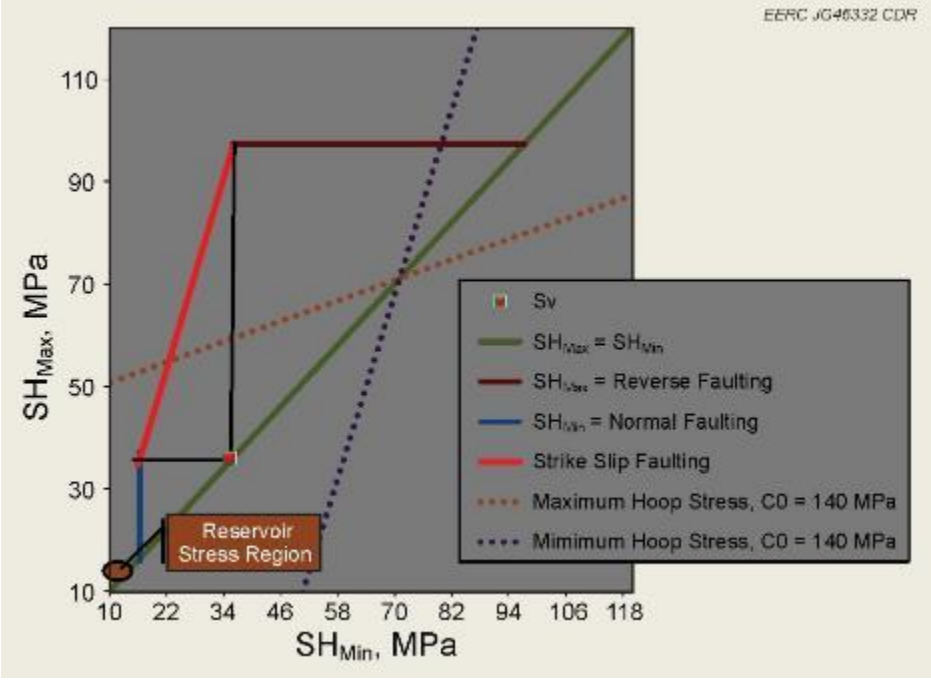

Figure 19. Stress polygon at initial reservoir conditions.

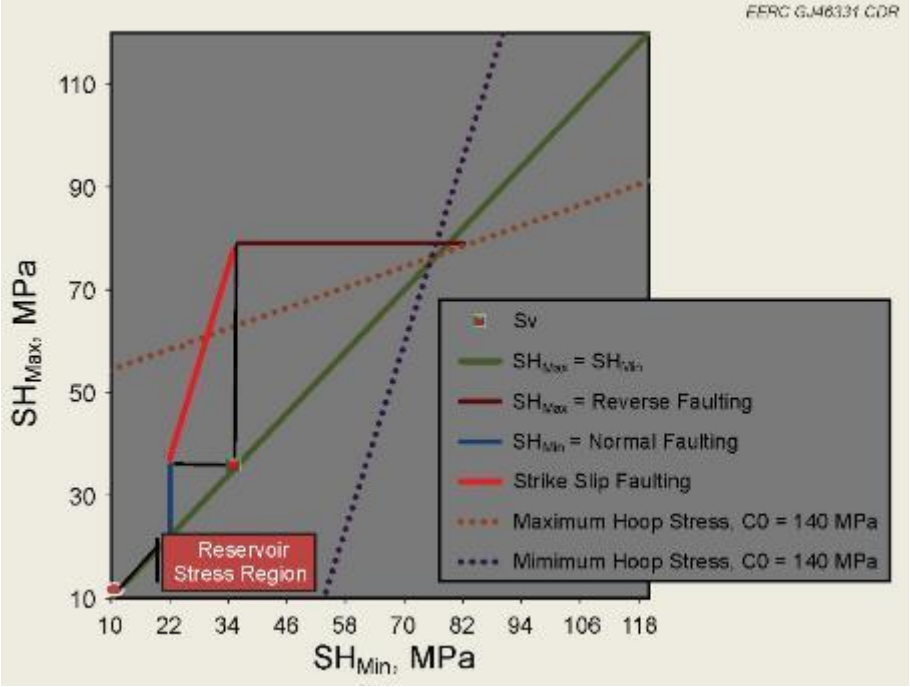

Figure 20. Stress polygon for reservoir conditions after injection.

Current and Future Work

3-D MEM Development

A 3-D MEM is currently being created for the Muddy Formation, including the upper and lower sealing formations, in order to assess the state of stress and reservoir mechanical properties present within the boundaries of the study area. The creation of a 3-D MEM will aid in the understanding of reservoir response to various stress states, which will make possible the prediction of formation deformation, permeability variation, and the maximum injection rate and pressure that can be utilized without compromising the integrity of the reservoir and confining units.

The 3-D MEM will be created based on the 1-D MEM, with the addition of 3-D seismic data, log data available throughout the field, newly acquired pulsed-neutron logs for wells in and around the Phase 1 zone, and core analysis. The 3-D MEM will contain a combination of stress states, geologic structure, seismic inversion-derived lithofacies, and reservoir elastic properties. The 3-D MEM can be used to monitor and predict dynamic changes throughout the field to assess and compare reservoir response to injection activities and monitoring data.

In addition to expanding the 1-D MEM into three dimensions, the 3-D MEM will be built to represent the entire Bell Creek Field. Once completed, this fieldwide 3-D MEM will be used as the initial condition for the geomechanical simulation model. The dynamic simulation of the rock mechanical properties and reservoir conditions will provide more accurate support for the

prediction of wellbore instability, fault reactivation, and potential leakage of CO_2 during the injection and storage process.

At the time of this writing, some work has been done on the fieldwide 3-D MEM. The structural framework of the geomechanical model was created by picking formation tops from the spontaneous potential and resistivity logs. Tops were picked from below the Muddy Formation, including the lower sealing formation, to the surface for wells inside and around the Bell Creek Field area. A total of 19 different zones, or 20 formation and member tops, were identified. The base of the model is the top of the Lakota Formation and extends upward to the ground surface.

Structural tops for formations overlying the reservoir were imported from the Bell Creek Petra database. Structural tops in the database included the Pierre, Shannon, Niobrara, Carlile, Mowry, Shell Creek, Springen Ranch, Muddy, Rozet, and Skull Creek. However, wells that had the SP and resistivity logs did not always have the tops for the above formations recognized. As a result, a well by well quality check was performed to ensure structural control of the model. This approach also allowed for the adjustment or creation of well tops that had been misplaced or unpicked.

Lithologically, most of the rock overlying the Bell Creek reservoir consists of Cretaceous shale. This can create difficulty when trying to differentiate formation tops when using only two logs as a reference. A limited amount of resources are available to help identify the different formations above the reservoir in Powder River and Carter Counties, Montana.

Fox (1993) identified formation tops from the SP and resistivity logs for Cretaceous-aged rocks commonly found in the Powder River Basin. Cross sections A-A' and B-B' from Fox (1993) extend through Powder River and Carter Counties and were utilized as a template to help identify structural tops for the geomechanical model. Additional tops added to the model that were not identified in the Petra database include the Turner Sandy Member and Pool Creek Member of the Carlile Formation, both identified by Fox (1993).

As shown in Figure 21, formation tops have been identified from signatures given by the SP and amplified short normal resistivity (ASN) logs from the surface to the base of the reservoir. After the tops were picked for each available well, structural surfaces were created and incorporated into a 3-D model in Petrel. The identification of the different formations and members helps identify geomechanical properties that are unique to each zone.

Currently, work is being done to correlate the rock mechanical data for the available wells in the Bell Creek oil field. The rock mechanical properties and stress states along those wells will be determined through the process of correlations and log synthetics. In addition, 3-D seismic data, which cover an area of 41 mi^2, will be available soon. A seismic inversion workflow will populate the 3-D MEM away from the wellbore.

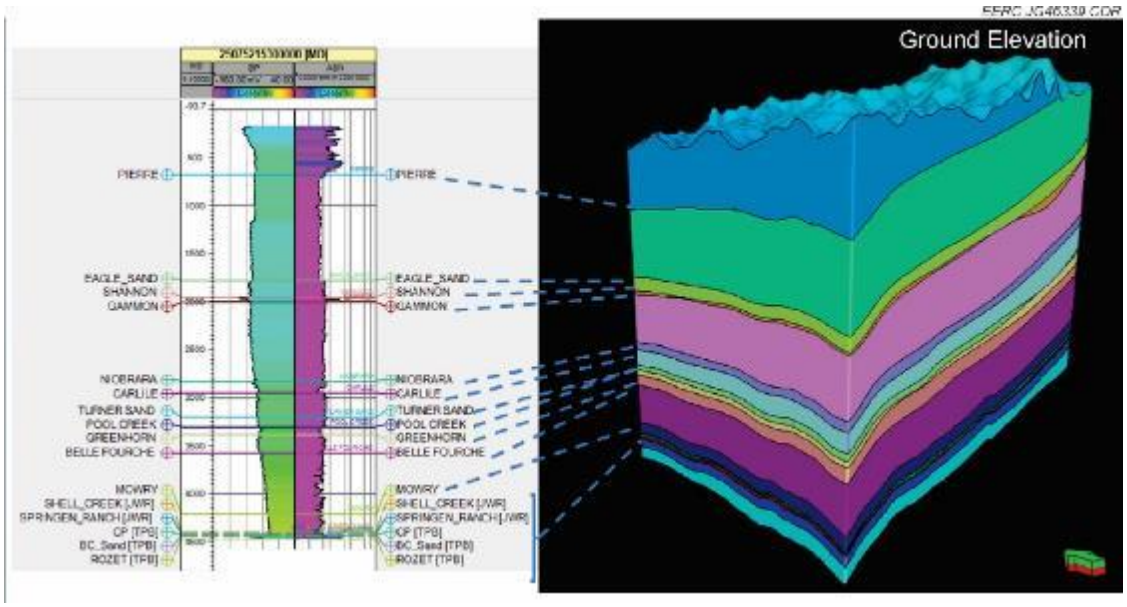

Figure 21. Well section window displaying structural tops, and 3-D cube displaying different geologic zones of the Bell Creek Field area.

The following approach will be used for data correlation and seismic inversion for the construction of the 3-D MEM:

- Proper correlations between the logs and the rock mechanical properties between wells will be researched to estimate the values of those properties and the in situ stress regimes of other wells.

- Correlations between the modeled stress regimes and rock mechanical properties for the 05-06 OW monitoring well and available logs will be carefully examined. Then, using the correlations, the properties for other wells in the Bell Creek Field will be estimated.

- Since the available log curves are different for each well, a synthetic process may be needed to create some logs for the correlations. In Techlog, this process was started using the module K.mod, which allows the user to model quantitative variables from one to several training data set(s). The module is based on the multilayer perceptron technology, a nonlinear regression statistical method (Figure 22).

- The 3-D seismic AVO (amplitude verse offset) inversion with well calibration will be performed with the 3-D seismic data. The seismic data will help estimate geomechanical properties away from the wellbore. The seismic inversion process will be performed using either Petrel or Hampson–Russell software packages. Methods in Petrel include genetic inversion using a stochastic seismic inversion plug-in and Earthworks seismic inversion plug-in. Multiple approaches may be used to compare results and the effectiveness of the various methods.

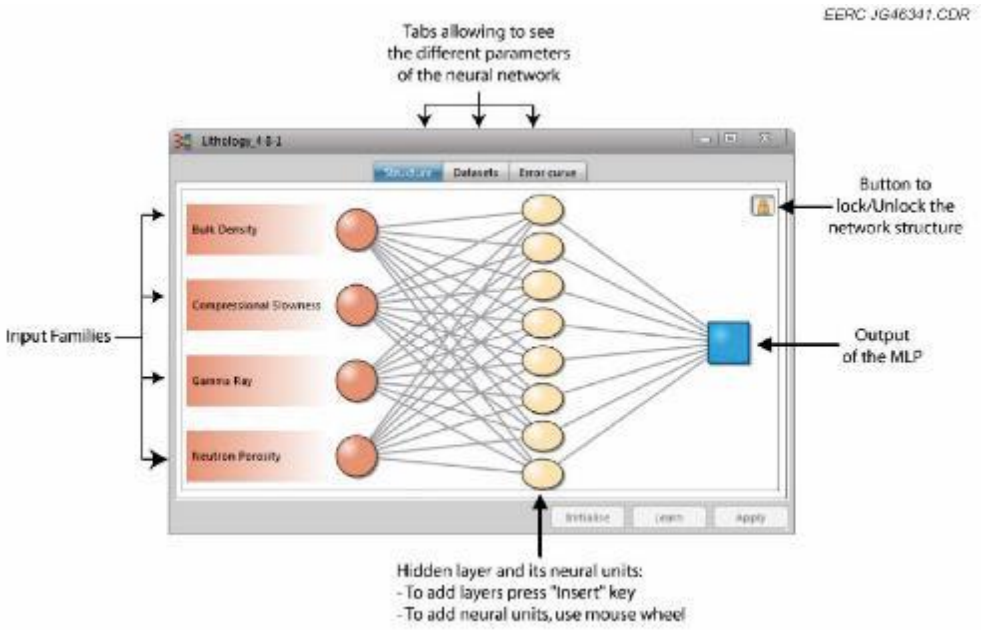

Figure 22. Neural network in K.mod (image from Techlog software).

The construction of the 3-D MEM will be finished in Petrel using the same frame as the geocellular model for the Bell Creek oil field. After well logs are correlated and the seismic AVO inversion process is completed, the estimated state of stress and rock mechanical properties will be extended into the entire field and beyond. All estimated property distributions will eventually be imported into Petrel and incorporated into the 3-D MEM. This static 3-D MEM will contain the reservoir, underburden, sideburden, and overburden to the surface.

Reservoir Geomechanical Simulation

When CO_2 is injected into the reservoir formation, it will affect the pressure and temperature and may change the stress and strain states in the formation. Those changes could then affect the porosity and permeability in the reservoir. The stress state is a coupled process between the reservoir properties and the mechanical rock properties and can affect not only the reservoir formations, but also the cap rock and all the formations to the surface. As a result, geomechanical simulation work will be performed following the completion of the fieldwide 3-D MEM. The goal of reservoir geomechanical simulation is to predict the CO_2 injection response to better guide monitoring efforts, predict the stress and strain variations in the reservoir formations and the cap rocks, and estimate the leakage potential for CO_2.

The current plan is to use FLAC3D™ as the geomechanical simulator, coupled with TOUGH2 or GEM (Computer Modelling Group Ltd.) as the reservoir simulator. Figure 23 shows the coupled simulation process using FLAC3D and TOUGH2.

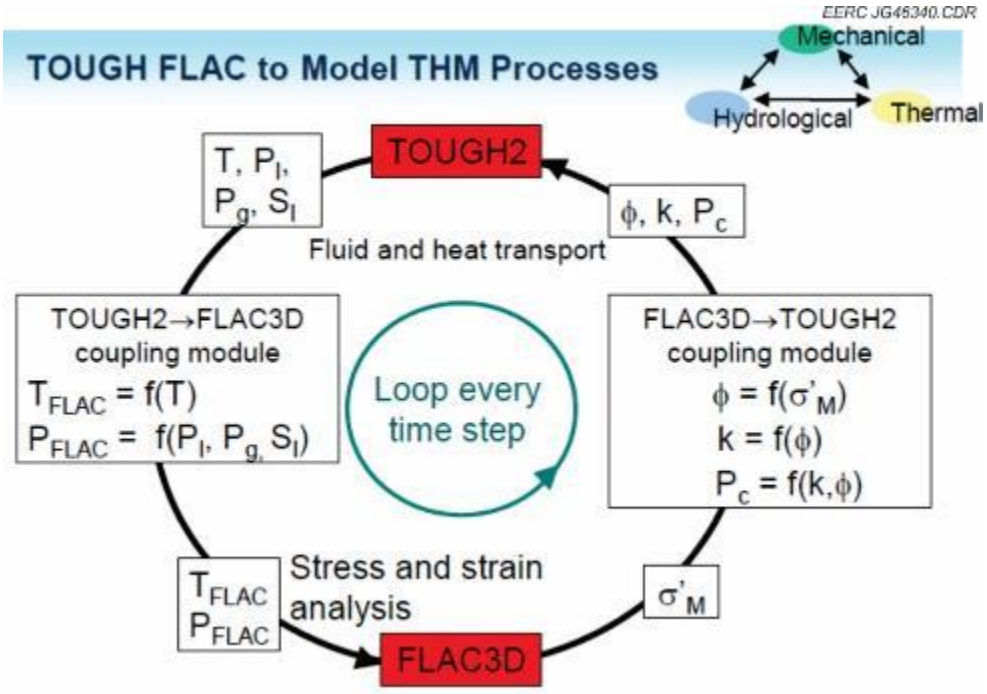

Figure 23. TOUGH2–FLAC3D simulation process (modified from Bodvarsson, 2005).

The simulation process will begin with the static 3-D MEM together with the reservoir properties in the 3-D geocellular model. The model will be imported from Petrel into the TOUGH2 reservoir simulator. Initial injection conditions, updated pressure of liquid and gas, and liquid saturation will be used to calculate reservoir pore pressure in a coupling module from TOUGH2 to FLAC3D. The updated reservoir pressure will be imported into the geomechanical simulator FLAC3D to predict the new state of stress and strain in the reservoir.

The updated porosity, permeability, and capillary pressure values can then be calculated in a coupled module of FLAC3D to TOUGH2 using the updated stress and strain information from FLAC3D. New porosity, permeability, and capillary pressure will be updated into the TOUGH2 reservoir simulator. This completes a single-time-step loop. A detailed workflow for the simulation work is being developed. The coupling module between FLAC3D and TOUGH2 is under construction in parallel with development of the 3-D MEM. Testing of the reservoir simulator TOUGH2 and the geomechanical simulator FLAC3D is being done. Another option for the coupled reservoir geomechanical simulation is GEM–FLAC3D. The simulation process would be similar to TOUGH2–FLAC3D, shown in Figure 23.

Conclusions

This report encompasses the completed, current, and future work with respect to geomechanical modeling efforts for the Bell Creek combined CO_2 EOR and CO_2 storage project. As an important supplement to the geocellular model, the 1-D MEM was built using Techlog and Petrel based on the data from the monitoring well (05-06 OW). Available data from the monitoring well were audited and processed, including log data and core-testing data. These data, along with

2-D seismic data, were used to construct the 1-D MEM model. The mechanical stratigraphy was constructed with the main lithology and facies from the reservoir formations to the ground surface. Rock mechanical properties and stress states along the monitoring well were estimated with the processed data from 1254 to 4732 ft. Above this interval, bulk density and vertical stress were estimated. These can be updated as additional data become available.

The fieldwide 3-D MEM is currently being constructed using the 1-D MEM and will be completed when additional log data and the 3-D seismic data become available. It is anticipated that the fieldwide 3-D MEM will be adjusted and incorporated with the new version of the geocellular model to better fit site-specific characteristics and evolving project needs. Furthermore, the geomechanical simulation work will be carried out once the 3-D MEM is completed.

Some preliminary results from analyses using the 1-D MEM include the predrilling wellbore stability and the stress polygons for determining the faulting regimes in the reservoir. Further analyses of injection safety and the potential for fluid leakage will be done as more information becomes available and after construction of the 3-D MEM.

KEY FINDINGS AND RECOMMENDATIONS

Key findings include the following:

- **1-D MEM** – Rock mechanical properties and stress states along the monitoring well were estimated.

- **Triaxial testing on core samples** – Results were used to verify the calculated results from the 1-D MEM for the Muddy Formation; however, because no data were obtained above the Muddy, these results could not be used to correlate the static and dynamic rock mechanical properties for these formations.

- **Horizontal stresses** – Caliper logs helped determine the orientations of horizontal stresses. The orientation of the maximum horizontal stress and the minimum horizontal stress are north–northeast–south–southwest and northwest–north–southeast–south, respectively. It should also be noted that the magnitudes of the minimum and maximum horizontal stresses in the region surrounding the monitoring well (05-06 OW) are nearly equal. This is further supported by only slight wellbore deformations that were observed (Figure 15) (the greater the difference in magnitude between these stresses, the higher the probability for large wellbore deformation and breakouts). The acquisition of additional data and construction of the 3-D MEM will help approximate these stresses throughout the rest of the field.

- **Wellbore stability analysis** – Based on the current 1-D MEM, the safe and stable mud weight windows were determined. The estimated maximum mud weight is 11.0567 PPG. No wellbore breakout will happen within the stable mud window, and this is corroborated by the fact that no breakouts have been found in the reservoir to date.

- **Induced faulting** – Preliminary stress polygon computations indicate that potential breakout through the reservoir as a result of drilling is extremely low.

Recommendations include the following:

- For more accurate core-to-log correlations, extra uniaxial and triaxial stress–strain measurements are highly recommended on core plugs.

- A whole-core high-definition computed tomography (CT) scan is recommended for deriving more information related to natural fractures in the reservoir.

- Minifracturing or leakoff testing is recommended for a more accurate estimation of the horizontal stress and tensile strength of the formation rocks.

It is highly recommended to use and update both the 1-D and 3-D MEMs during the drilling of new wells in the field and as new data and simulation results become available. These models will be used to provide insight into the site-specific geomechanical changes associated with stress, strain, pressure, permeability, and porosity resulting from the injection of CO_2; predict potential leakage; constrain the injection pressure; optimize the injection plan; simulate the movement of CO_2 in the subsurface; and predict potential induced seismic events. An accurate understanding of these issues will help support decision making.

REFERENCES

Afsari, M., Amani, M., Razmgir, S.M., Karimi, H., and Yousefi, S., 2010, Using drilling and logging data for developing 1-D Mechanical Earth Model for a mature oil field to predict and mitigate wellbore stability challenges. SPE 132187. www.onepetro.org/mslib/servlet/onepetropreview?id=SPE-132187-MS (accessed January 2013).

Bodvarsson, G.S., 2005, Presentation on the Yucca Mountain project – computer modeling of ambient and thermal processes.

Crain, E.R., 2013a, www.spec2000.net/10-elastic.htm (accessed June 2013).

Crain, E.R., 2013b, www.spec2000.net/10-closurestress.htm (accessed June 2013).

Eaton, B.A., 1969, Fracture gradient prediction and its application in oilfield operations, Journal of Petroleum Technology, October, p. 1350–1360, www.onepetro.org/mslib/servlet/onepetropreview?id=00002163 (accessed December 2012).

Fox, J.E., 1993, Stratigraphic cross sections A-A through F-F showing electric logs of Upper Cretaceous and older rocks, Powder River Basin, Montana and Wyoming: U.S. Geological Survey Oil and Gas Investigations Chart OC-135.

Gale, J.F.W., Reed, R.M., and Holder, J., 2007, Natural fractures in the Barnett Shale and their importance for hydraulic fracture treatments: AAPG Bulletin, v. 91, no. 4, p. 603–622 www.beg.utexas.edu/starr/PDF/Gale/Gale_et_al_Natural_2007.pdf (accessed June 2013).

Khan, S., Han, H., Ansari, S., and Khosravi, N., 2010, An integrated geomechanics workflow for cap rock integrity analysis of a potential carbon storage site. International Conference on CO_2 Capture, Storage, and Utilization: New Orleans, Louisiana, November 10–12 (SPE 139477).

Nagy, Z.S., Pacheco, F., Rosa, M., Riberro, M., Jouti, I., Pastor, J., Grandy, A., Fluckiger, S., and Gigena, L., 2011, Use of geomechanics for optimizing reservoir completion and stimulation strategies for carbonates in the Campos Basin, Offshore Brazil, Offshore Technology Conference: Rio De Janeiro, Brazil, October 4–6, OTC 22364.

Plumb, R., Edwards, S., Pidcock, G. Lee, D., and Stacey, B., 2000, The Mechanical Earth Model concept and its application to high-risk well construction projects. 2000 IADC/SPE Drilling Conference: New Orleans, Louisiana, February 23–25, SPE 59128.

Rutqvist, J., 2008, Geomechanical modeling associated with geological CO_2 sequestration, Lawrence Berkeley National Laboratory.

Sayers, C., Russell, C., Pelorosso, M., Adachi, J., Pastor, J., Singh, V., Tagbor, K., and Hooyman, P., 2009, Determination of rock strength using advanced sonic log interpretation techniques: presented at the 2009 SPE ATCE, New Orleans, Louisiana, October 4–7.

BIBLIOGRAPHY

Bostrom, B., 2009, Development of a geomechanical reservoir modeling workflow and simulations. SPE Annual Technical Conference and Exhibition: New Orleans, Louisiana, October 4–7.

Bradford, I.D.R., Fuller, J., Thompson, P.J., and Walsgrove, T.R., 1998, Benefits of assessing the solids production risk in a North Sea reservoir using elastoplastic modeling. SPE/ISRM Eurock ’98: Trondheim, Norway, p. 261–269.

Computer Modelling Group Ltd., 2011, CMG’s GEM user’s guide: Calgary, Alberta, Computer Modelling Group, 1246 p.

Encore Acquisition Company, 2009, Bell Creek CO_2 project: Internal report, 8 p.

Orlic, B., Heege, J.H., and Van Thienen-Visser, K., 2010, Results of preliminary simulations of the impact of CO_2 injection on generic models, CATO-2 Deliverable WP3.03-D02.

Saini, D., Braunberger, J.R., Pu, H., Bailey, T.P., Ge, J., Crotty, C.M., Liu, G., Hamling, J.A., Gorecki, C.D., Steadman, E.N., and Harju, J.A., 2012, Bell Creek test site – simulation report: Plains CO_2 Reduction (PCOR) Partnership Phase III draft Task 9 Deliverable D66 executive

summary for U.S. Department of Energy National Energy Technology Laboratory Cooperative Agreement No. DE-FC26-05NT42592, Grand Forks, North Dakota, Energy & Environmental Research Center, August.

Sinha, B.K., Vissapragada, B., Renlie, L., and Skomedal, E., 2006, Horizontal stress magnitude estimation using the three shear moduli – A Norwegian Sea case study: presentation at the 2006 SPE ATCE, San Antonio, Texas, September 24–27.

Sorensen, J.A., Smith, S.A., Lindeman, C.D., Steadman, E.N., and Harju, J.A., 2010, Bell Creek test site – geomechanical experimental design package: Plains CO_2 Reduction (PCOR) Partnership Phase III Task 4 Deliverable D87 for U.S. Department of Energy National Energy Technology Laboratory Cooperative Agreement No. DE-FC26-05NT42592, EERC Publication 2011-EERC-06-13, Grand Forks, North Dakota, Energy & Environmental Research Center, October.

Soroush, H., 2010, Importance of petrophysical logging data to geomechanical analysis: presentation at SPWLA, the Abu Dhabi Chapter.

Vuke, S.M., 1984, Depositional environments of the Early Cretaceous Western Interior Seaway in southwestern Montana and the northern United States, in Stott, D.F., and Glass, D.J., eds., The Mesozoic of Middle North America: Canadian Society of Petroleum Geologists, Memoir 9, p. 127–144.

Weimer, R.J., Emme, J.J., Farmer, C.L., Anna, L.O., Davis, T.L., and Kidney, R.L., 1982, Tectonic influence on sedimentation, Early Cretaceous, east flank Powder River Basin, Wyoming and South Dakota: Colorado School of Mines Quarterly, v. 77, no. 4.

Wulf, G.R., 1962, Lower Cretaceous Albian rocks in northern Great Plains: American Association of Petroleum Geologists Bulletin, v. 46, no. 8, p. 1372–1415.

Young, R.G., 1970, Lower Cretaceous of Wyoming and the southern Rockies: Mountain Geologist, v. 7, p. 105–121.

Zandi, S., Renard, G., and Nauroy, J.F., 2010, Numerical coupling of geomechanics and fluid flow during steam injection in SAGD, SPE 129739.

Zoback, M.D., Barton, C.A., Brudy, M., Castillo, D.A., Finkbeiner, T., Grollimund, B.R., Moos, D.B., Peska, P., Ward, C.D., and Wiprut, D.J., 2003, Determination of stress orientation and magnitude in deep wells: International Journal of Rock Mechanics and Mining Sciences, v. 40, p. 1049–1076.

APPENDIX A

APPROACHES FOR DATA INTERPRETATION AND MODELING ACTIVITIES

APPROACHES FOR DATA INTERPRETATION AND MODELING ACTIVITIES

The following approaches were used for data interpretation and modeling activities.

Rock elastic mechanical properties were estimated using the sonic velocity log data from the 05-06 OW monitoring well.

Young's Modulus (E): The dynamic Young's modulus of rock is given by the following equation:

$$E_{dyn} = \frac{RHOB\, V_s^2 (3V_p^2 - 4\, V_s^2)}{(V_p^2 - V_s^2)} \quad \text{[Eq. 1]}$$

in which, *RHOB* is the bulk density, V_p is the compressional elastic waves, and V_s is the shear elastic waves.

The static Young's Modulus was converted from the dynamic Young's modulus by empirical or experimental equations, for example, the generally used Wang correlation (unit in GPa) for soft rocks (Wang, 2000; Sayers et al., 2009):

$$E_{sta} = 0.4145 E_{dyn} - 1.0593 \quad \text{[Eq. 2]}$$

In this work, a correlation between the static and dynamic Young's modulus was also done with the results from triaxial tests to estimate the static Young's modulus. Results can be compared to determine the better method for the Bell Creek Field.

Unconfined Compressive Strength (UCS): The Plumb empirical correlation was used for the estimation of UCS (unit in MPa, note that E_{sta} is in GPa) based on dipole sonic data (Bradford and others, 1998):

$$UCS = 2.280 + 4.1089\, E_{sta} \quad \text{[Eq. 3]}$$

A correlation between the static Young's modulus and UCS was also done with the results from triaxial tests to estimate the UCS.

Poisson's Ratio (v): The estimation of the dynamic Poisson's ratio is given by the following equation:

$$v_{dyn} = \frac{(V_p^2 - 2V_s^2)}{2(V_p^2 - V_s^2)} \quad \text{[Eq. 4]}$$

The static Poisson's ratio was converted from the dynamic Poisson's ratio available from the 05-06 OW dipole sonic log through the correlation (Afsari and others, 2010):

$$v_{sta} = 0.7 v_{dyn} \quad \text{[Eq. 5]}$$

In this project, with the results from the triaxial tests, another correlation was given for the static and dynamic Poisson's ratio.

Friction Angle (ø): Values of 35º and 25º were used for carbonate-dominant and shale-dominant zones, respectively (Afsari and others, 2010).

Lithology Analysis was based on spectral gamma ray, bulk density, neutron porosity, capture spectroscopy, and DTCO (compressional wave transit time, V_p) logs to determine the dominant lithology, i.e., sandstone or shale.

In Situ Stress Analysis

Both the magnitude and direction of the in situ stresses should be estimated before construction of the 1-D mechanical earth model (MEM). The following techniques were used for determining the parameters.

Vertical Stress (σ_v): The magnitude of vertical stress in Well 05-06 OW was computed by integrating formation density (RHOB log) through the overburden (Zoback and others, 2003).

$$\sigma_v = \int_0^z \rho\,(z) g\, dz \qquad \text{[Eq. 6]}$$

Pore Pressure can be predicted by a modular formation dynamics tester, DTCO, and/or resistivity logs. The Eaton method was used for the estimation of pore pressure (Eaton, 1969). A pore pressure log is available from the 05-06 OW monitoring well and was used to verify the pore pressure prediction results. The pressure gauge data from the monitoring well were also used for the modification of pore pressure:

$$P_p = \sigma_v - \left(\sigma_v - P_{p,n}\right)\left(\frac{V_p}{V_{p,n}}\right)^3 \qquad \text{[Eq. 7]}$$

in which, $P_{p,n}$ is the normal hydrostatic pressure, and $V_{p,n}$, which is the normal trend of V_p, can be found through constructing the proper trend line for V_p (as shown in Figure A-1 for the V_p from the monitoring well).

Then the verified log for σ_v was utilized to calculate the minimum horizontal stress.

Minimum Horizontal Stress (σ_h): The magnitude of the minimum horizontal stress can be determined by the elastic properties, v, E, and α (Biot's coefficient) equation (Afsari and others, 2010):

$$\sigma_h = \frac{v}{1-v}\left(\sigma_v - \alpha P_p\right) + \alpha P_p + \frac{E_{sta}}{1-v^2} e_{H,\ min} + \frac{v\, E_{sta}}{1-v^2} e_{H,\ max} \qquad \text{[Eq. 8]}$$

in which E_{sta} is the static Young's modulus, $e_{H,\ min}$ is the minimum horizontal strain, and $e_{H,\ max}$ is the maximum horizontal strain. In this case, the strains were considered negligible because of their relatively small values.

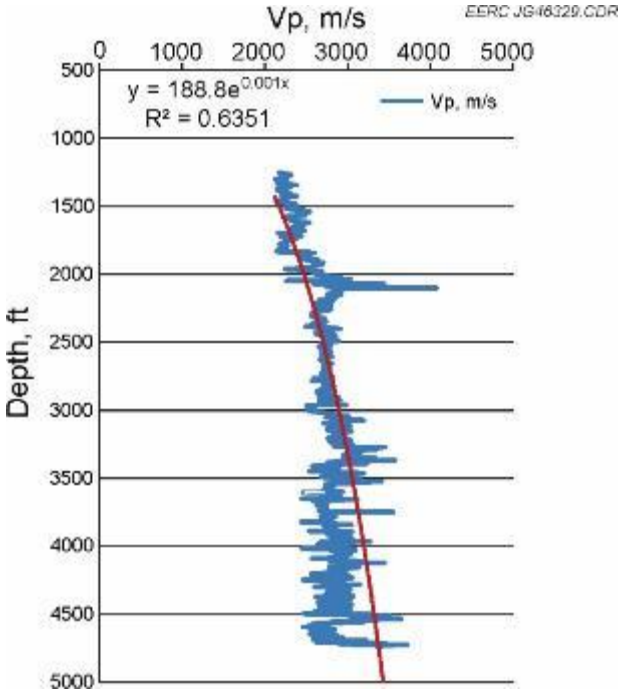

Figure A-1. Normal trend of the velocity log for monitoring well.

Maximum Horizontal Stress (σ_H): The magnitude of the maximum horizontal stress cannot be measured or computed directly. A constrain modeling technique (Moos and Zoback, 1990; Zoback and others, 2003) can be used to constrain the maximum horizontal stress with key mechanical parameters (including vertical stress, minimum horizontal stress, Young's modulus, Poisson's ratio, Biot's coefficient, local fault type, induced fracture, or wellbore breakout direction). The Mohr–Coulomb failure criterion can then be utilized to adjust the maximum horizontal stress so that the model can reproduce the failure observed in specific failure intervals. XRMI log data can be used for failure criterion to constrain the magnitude and direction of the maximum horizontal stress. The borehole failure on image logs could be used to determine the direction of horizontal stresses.

The constrain models used for the estimation of the magnitude of maximum horizontal stress were summarized by Soroush (2010) respective to different available data. Those methods include constrain models using tensile fractures, using borehole breakouts, or using wellbore and rock strength (Soroush, 2010).

Besides the constrain model for the estimation of the magnitude of the maximum horizontal stress, other methods include the following:

1. From hydraulic fracturing analysis:

$$\sigma_H = \frac{v}{1-v}\left(\sigma_v - \alpha P_p\right) + \alpha P_p + \sigma_{tect} \qquad \text{[Eq. 9]}$$

in which, the σ_{tect} is the tectonic stress contribution.

2. From in situ stress configuration:

$$\sigma_H = \frac{(\sigma_h - \alpha P_p)}{v} - \sigma_v + 2\alpha P_p \quad \text{[Eq. 10]}$$

3. From three shear moduli (Sinha and others, 2006):

$$\sigma_H = \sigma_h + \frac{(C_{55} - C_{44})}{A_E} \quad \text{[Eq. 11]}$$

$$C_{44} = \frac{\rho}{DT_{fs}^2} \quad \text{[Eq. 12]}$$

$$C_{55} = \frac{\rho}{DT_{ss}^2} \quad \text{[Eq. 13]}$$

$$C_{66} = \frac{\rho_{mud}}{(1/DT_{tube}^2 + 1/DT_{mud}^2)} \quad \text{[Eq. 14]}$$

$$A_E = \frac{(C_{55} - C_{66})}{S_v - \sigma_h} \quad \text{[Eq. 15]}$$

in which C_{44} is fast dipole shear moduli, C_{55} is slow dipole shear moduli, A_E is an acousto-elastic parameter, and C_{66} is Stoneley-derived horizontal shear modulus (Buffin and others, 2008).

These methods can be tested for maximum horizontal stress with more data available. The MEM can be updated with more data and accurate methods.

To use Equations 1–5 for the estimation of rock mechanical properties, the sonic logs were converted to velocity logs. All of these logs were finally converted into the same unit system as the bulk density log. After data preparation, the mechanical properties of the rocks were then calculated using Equations 1–5. Among those equations, Equations 2, 3, and 5 are empirical correlations between variables. Correlations were made based on the core analysis results from the triaxial tests.

Figure A-2 shows the correlation between the static and dynamic Young's modulus (Sample 49V was neglected intentionally for the Young's modulus correlation because of its especially low static value). From the trend line on the figure, a linear correlation between static and dynamic Young's modulus was determined:

$$E_{sta} = 0.2396E_{dyn} + 3.9464 \quad \text{[Eq. 16]}$$

For the estimation of the UCS: the Plumb empirical correlation can only be accurate for the sandstone. The static Young's modulus from the triaxial test results was correlated with UCS (Figure A-3). The correlation can be expressed as follows:

$$UCS = 0.0033E_{sta} + 0.0228 \quad \text{[Eq. 17]}$$

The correlation between the static Poisson's ratio and the dynamic Poisson's ratio was also done using the results from the triaxial tests. The linear correlation is shown in Figure A-4, and the empirical correlation can be expressed as follows:

$$v_{sta} = 0.7142 v_{dyn} + 0.0443 \quad \text{[Eq. 18]}$$

The linear correlations shown in Equations 16–18 and Figures A-2–A-4 indicate a possible relationship between static and dynamic Poisson's ratio. It would be beneficial to have two or three more triaxial test results on each lithology facies, because the correlation of two properties could be different for different lithologies. These linear correlations were used as reference log curves in the 1-D MEM.

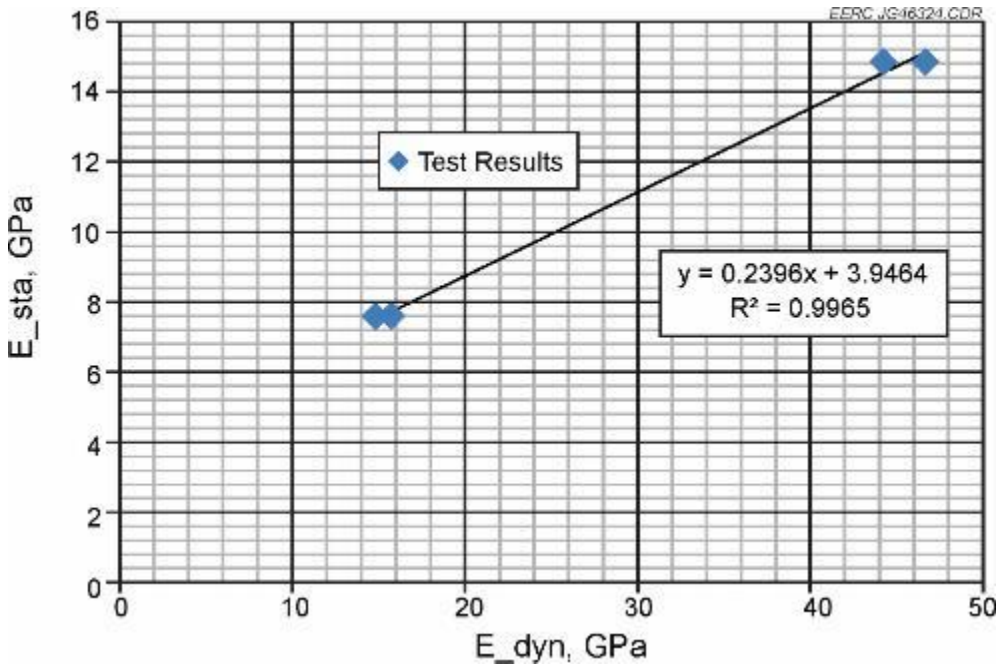

Figure A-2. Correlation between E_dyn and E_sta using the triaxial test results.

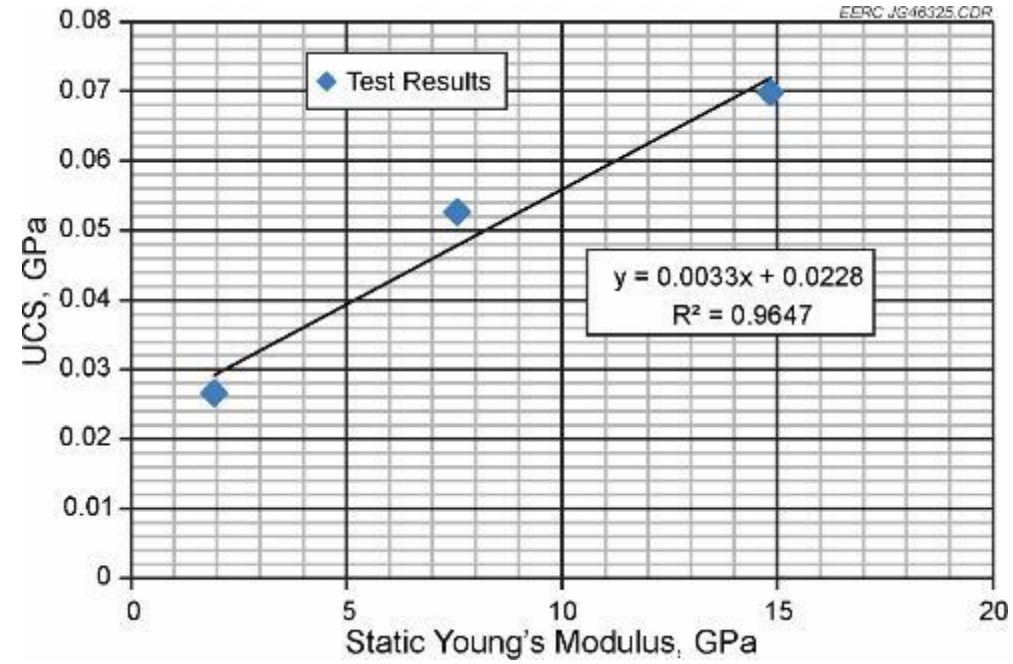

Figure A-3. Correlation between UCS and E_sta using the triaxial test results.

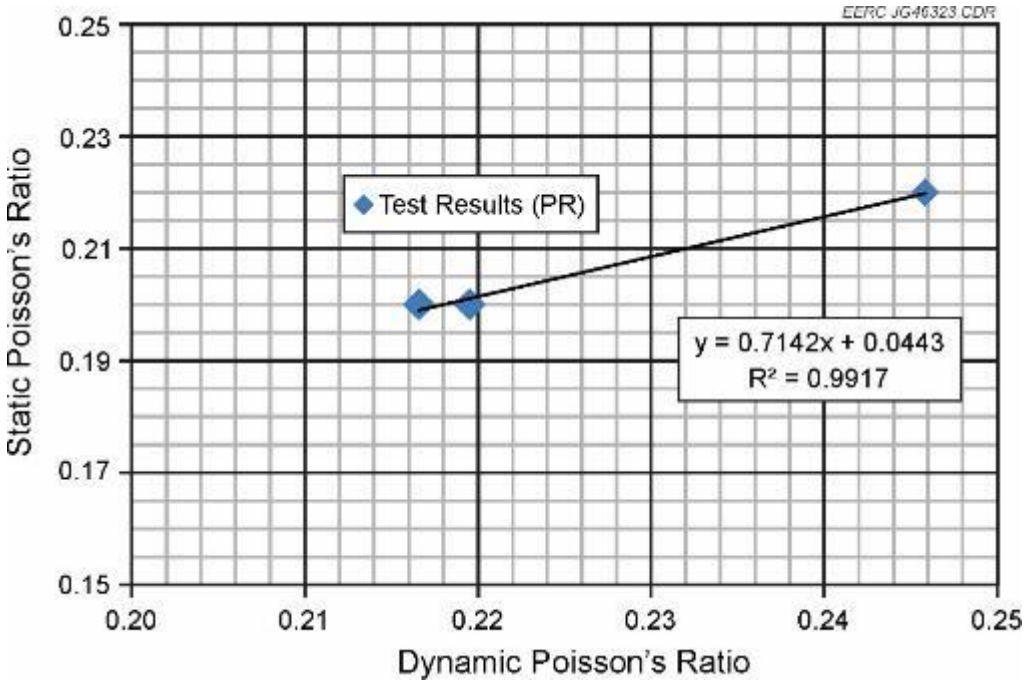

Figure A-4. Correlation between static and dynamic Poisson's ratio.

REFERENCES

Afsari, M., Amani, M., Razmgir, S.M., Karimi, H., and Yousefi, S., 2010, Using drilling and logging data for developing 1-D Mechanical Earth Model for a mature oil field to predict and mitigate wellbore stability challenges. SPE 132187, www.onepetro.org/mslib/servlet/onepetropreview?id=SPE-132187-MS (accessed January 2013).

Bradford, I.D.R., Fuller, J., Thompson, P.J., and Walsgrove, T.R., 1998, Benefits of assessing the solids production risk in a North Sea reservoir using elastoplastic modeling. SPE/ISRM Eurock '98: Trondheim, Norway, p. 261–269.

Buffin, A., Avila, J., John, Z., Sinha, B., and Tan, C., 2008, A new approach in building a mechanical earth model using acoustically derived shear moduli: Woodside and Schlumberger Presentation, April 12: www.fesaus.org/download/SPWLA_BANGKOK_PAPER_for_presentation_Ver-22Aug2008.pdf (accessed January 2013).

Eaton, B.A., 1969, Fracture gradient prediction and its application in oilfield operations, Journal of Petroleum Technology, October, p. 1350–1360, www.onepetro.org/mslib/servlet/onepetropreview?id=00002163 (accessed December 2012).

Moos, D., and Zoback, M., 1990, Utilization of observations of well bore failure to constrain the orientation and magnitude of crustal stresses: Applications to continental, Deep Sea drilling project, and ocean drilling program boreholes. Journal of Geophysical Research 95(B6): doi: 10.1029/90JB00495, ISSN: 0148-0227.

Sayers, C., Russell, C., Pelorosso, M., Adachi, J., Pastor, J., Singh, V., Tagbor, K., and Hooyman, P., 2009, Determination of rock strength using advanced sonic log interpretation techniques: presented at the 2009 SPE ATCE, New Orleans, Louisiana, October 4–7.

Sinha, B.K., Vissapragada, B., Renlie, L., and Skomedal, E., 2006, Horizontal stress magnitude estimation using the three shear moduli – A Norwegian Sea case study: presentation at the 2006 SPE ATCE, San Antonio, Texas, September 24–27.

Soroush, H., 2010, Importance of petrophysical logging data to geomechanical analysis, presentation at SPWLA, the Abu Dhabi Chapter.

Wang, Z., 2000, Dynamic versus static elastic properties of reservoir rocks: Tulsa, Society of Exploration Geophysicists, *in* Wang, Z., and Nur, A.M., eds., Seismic and Acoustic Velocities in Reservoir Rocks: Tulsa, Society of Exploration Geophysicists, v. 3, p. 531–539.

Zoback, M.D., Barton, C.A., Brudy, M., Castillo, D.A., Finkbeiner, T., Grollimund, B.R., Moos, D.B., Peska, P., Ward, C.D., and Wiprut, D.J., 2003, Determination of stress orientation and magnitude in deep wells: International Journal of Rock Mechanics and Mining Sciences, v. 40, p. 1049–1076.

APPENDIX B

METHOD TO GENERATE P-WAVE VELOCITY DATA

METHOD TO GENERATE P-WAVE VELOCITY DATA

A useful method to generate P-wave velocity data was applied by resistivity–velocity transforms (Figure B-1). Based on the fact that resistivity data such as deep induction log are available in most of the wells from surface to reservoir depth, it can be used to generate sonic logs from the surface. It is very important to first validate results in wells with available sonic data. Different available transforms in the literature have been applied to the monitoring well to check for the best results in our analysis.

Shear wave (S-wave) velocity is also needed to estimate Poisson's ratio and Young's modulus in each well. Many methods exist to estimate S-wave velocity, and each method can be used depending on data availability. One method uses crossplots with P-wave data to find a general relationship. Figures B-1 to B-3 represent the P–S wave relationship in the monitoring well of the reservoir section (Bell Creek sand) from the sonic log.

Two different methods exist to find the most reliable transform between P–S waves:

1) Using monitoring well P- and S-wave velocity log data (Figure B-2).

2) Lab measurements: P- and S-wave velocity can be measured on core plug samples, and the transforms can be generated and applied in general.

To find the best correlation in the above steps, generating the best regression between the data, analysis of variance test and regression analysis are performed to choose the governing factors in each correlation.

With the modified P and S waves for the reservoir conditions (Figure B-3), the adjusted stress states for the reservoir formations were calculated as shown in Table B-1.

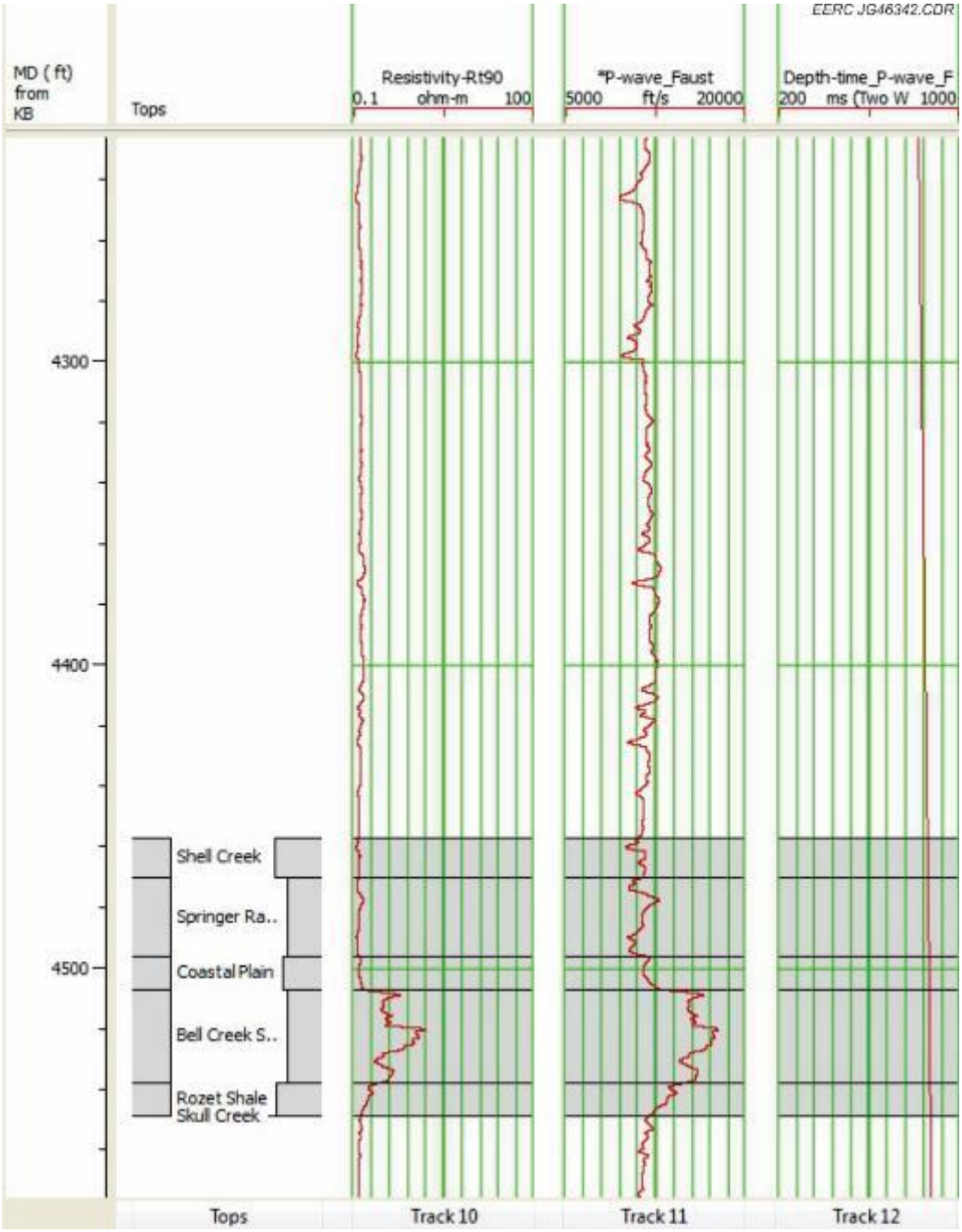

Figure B-1. Resistivity–velocity generation for validating the data in monitoring well with modified Faust correlation.

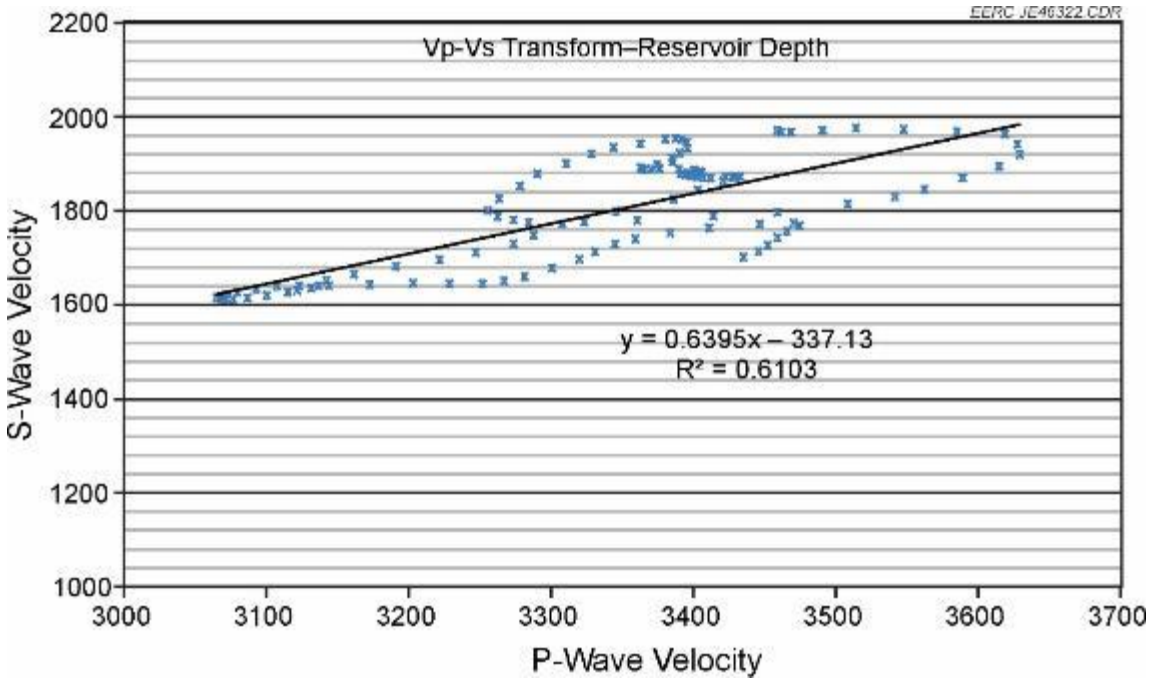

Figure B-2. P–S waves transform.

Table B-1. Adjusted Stress State for the Reservoir Formations

	Depth	SigmV, psi	PP, psi	PR	SH_{min}, psi	SH_{max}, psi
CP	4502.50	5387.60	1046.83	0.33	3225.69	3402.45
BC10	4513.00	5087.38	1049.27	0.33	3024.73	3173.70
BC20	4523.50	5253.28	1051.72	0.28	2680.80	2761.01
BC30	4534.50	5147.00	1054.27	0.27	2547.36	2681.92
Rozet	4542.00	5604.14	1056.02	0.34	3361.61	3423.33

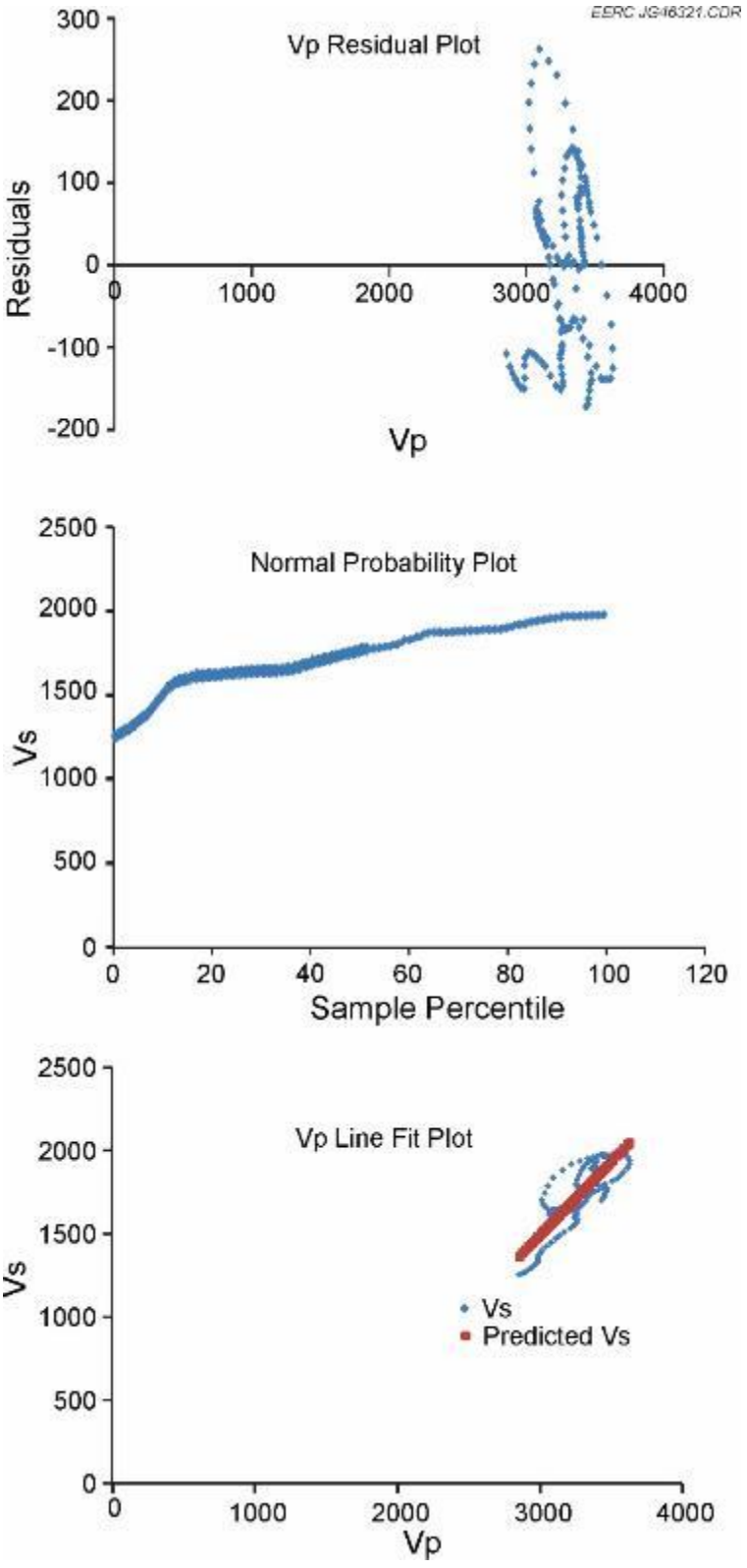

Figure B-3. S-wave prediction process.